Theoretical Advances toward Understanding Recent Experiments in Biophysical Chemistry

by

Eric Norman Zimanyi

B.Sc., McGill University (2006)

Submitted to the Department of Chemistry
in partial fulfillment of the requirements for the degree of

Doctor of Philosophy

at the

MASSACHUSETTS INSTITUTE OF TECHNOLOGY

June 2012

Author .....
Department of Chemistry
May 9, 2012

Certified by .....
Jianshu Cao[1]
Professor of Chemistry

Accepted by .....
Robert W. Field
Chairman, Department Committee on Graduate Theses

[1]On behalf of Robert J. Silbey, Class of 1942 Professor of Chemistry, Thesis Supervisor

This thesis has been examined by a Committee of the Department of Chemistry as follows:

Professor Troy Van Voorhis .....
Chairman, Thesis Committee
Associate Professor of Chemistry

Professor Jianshu Cao .....
Professor of Chemistry

Professor Irwin Oppenheim .....
Professor Emeritus of Chemistry

Theoretical Advances toward Understanding Recent Experiments in Biophysical Chemistry

by

Eric Norman Zimanyi

Submitted to the Department of Chemistry
on May 9, 2012, in partial fulfillment of the
requirements for the degree of
Doctor of Philosophy

Abstract

Several theoretical advances are presented, with the common theme of helping better understand and guide recent experiments in biophysical chemistry. In Chapter 2, I consider a recent criticism of the Jarzynski equality, notably that a breakdown in the connection between work and changes in the Hamiltonian for time-dependent systems causes the Jarzynski equality to produce unphysical results. I discuss the relationship between two possible definitions of free energy and demonstrate that it is indeed possible to obtain physically relevant free energy profiles from the Jarzynski equality, thereby resolving the recent questions in the literature. Next, I consider several aspects of coherent resonance energy transfer. In Chapter 3, I present a theory for coherent resonance energy transfer based on classical electrodynamics and demonstrate how it is able to capture dynamics in the coherent regime, the incoherent regime, and in between these two limits. In Chapter 4, I present a quantum theory for resonant energy transfer based on using a variational polaron transform to optimally split the Hamiltonian into a zeroth-order part and a perturbation. I then apply a quantum master equation to obtain the dynamics of energy transfer for various parameters. Finally, in Chapter 5, I examine whether it is possible to use the known exact equilibrium state of the system to improve the variational procedure.

Thesis Supervisor: Robert J. Silbey
Title: Class of 1942 Professor of Chemistry

Acknowledgments

First of all, I would like to thank my advisor, Prof. Robert Silbey, for the advice and encouragement he gave me over the course of my studies. While his service to the School of Science and to the entire MIT community is well known throughout the institute, he excelled just as much in his role as a research advisor. He was always available to discuss my progress, and provided countless helpful and insightful suggestions. While he is not here to see this finished product, he played a large part in the research described here and his influence is present throughout this thesis. I am privileged to have had the opportunity to work with him. I would also like to thank the numerous members of the chemistry faculty who went out of their way to make sure I had the support I needed in my final months here.

There are many people with whom I have had interesting and stimulating discussions about the work presented here. I would like to acknowledge Prof. Chris Jarzynski for providing some useful comments on the work presented in Chapter 2. I thank Ahsan Nazir and Dara McCutcheon for many useful discussions about variational master equations. Finally, I would like to thank Cheekong Lee and Jeremy Moix for providing the equilibrium data on which Chapter 5 is based. In addition, I thank Steve Pressé for our many useful and stimulating discussions, both while he was at MIT and in the years since.

I thank my thesis committee, Profs. Irwin Oppenheim, Jianshu Cao, and Troy Van Voorhis, for their input on my work over the years. My interactions with them went far beyond the prescribed annual meetings, and I have learned a great deal from our many discussions. I would also like to thank all of my colleagues in the zoo for providing an enjoyable and intellectually stimulating work environment.

During the majority of my time at MIT, I was partially funded by the Fonds québécois de la recherche sur la nature et les technologies, and I gratefully acknowledge this support.

I would also like to thank my friends in Boston who made my time outside of MIT enjoyable; in particular, I shared many good times with Peter, Emily, Marc, Katie,

Becca, and Arturo. My family has always supported me in my academic endeavors, and I thank Mum, Dad, Lisa, and Kevin for their support during my years in graduate school. Finally, and above all, I thank Christina for being a constant source of support and encouragement over the past few years.

Contents

1 Introduction **15**

2 Jarzynski Equality **23**

2.1 Introduction 23

2.2 Choice of system and environment 27

2.3 Description of pulling experiment 30

2.4 Conclusion 35

3 Classical Energy Transfer **41**

3.1 Introduction 41

3.2 Classical theory 44

3.3 Quantum mechanical theory 50

3.4 Results 57

3.5 Conclusion 67

3.6 Appendix—Static Approximation 68

4 Variational polaron transform **75**

4.1 Introduction 75

4.2 Perturbations 79

4.3 Model 82

4.4 Variational polaron transform 84

4.4.1 Partial polaron transform 84

4.4.2 Variational condition 86

4.5 Perturbative solution of dynamics 87
4.5.1 Overview 87
4.5.2 Correlation functions 88
4.5.3 Commutators 90
4.6 Results 92
4.6.1 Ohmic bath 92
4.6.2 Superohmic bath 97
4.7 Conclusion 101

5 Alternative Variational Transformations 109

5.1 Introduction 109
5.2 Polaron transformation 110
5.3 Results 114
5.4 Conclusion 116

List of Figures

3-1 Fraction of energy transferred as a function of time for a donor with a single excited state $\hbar\omega_d = 1.6600$ eV and an acceptor with a single excited state $\hbar\omega_a = 1.6539$ eV. Parameters: $r = 9$ Å, $\epsilon = \epsilon_0$, all transition dipole moments are 1 in atomic units. The radiative decay rate is $(80\text{ ns})^{-1}$ for all dipoles in the classical model; no radiative decay is included in the quantum model. The solid line is calculated using quantum mechanics and the circles are calculated using our classical method. 59

3-2 Fraction of energy transferred as a function of time for a donor with a single excited state $\hbar\omega_d = 1.66$ eV and an acceptor with a continuum of 75 excited states evenly spaced in the range $\hbar\omega_a = 1.635$ eV to $\hbar\omega_a = 1.685$ eV. The transition dipole moments are 1 for the donor and 0.1 for all acceptor states. Parameters: $r = 9$ Å, $\epsilon = \epsilon_0$. The radiative decay rate is $(80\text{ ns})^{-1}$ for all dipoles in the classical model; no radiative decay is included in the quantum model. The solid line is calculated using quantum mechanics and the circles are calculated using our classical method. 60

3-3 Fraction of energy transferred as a function of time for a donor with a single excited state $\hbar\omega_d = 1.66$ eV and an acceptor with a continuum of 75 excited states evenly spaced in the range $\hbar\omega_a = 1.635$ eV to $\hbar\omega_a = 1.685$ eV. The transition dipole moments are 1 for the donor and 0.1 for all acceptor states, except the acceptor state at $\hbar\omega = 1.6539$ eV which has a transition dipole moment of 1. Parameters: $r = 9$ Å, $\epsilon = \epsilon_0$. The radiative decay rate is $(80\text{ ns})^{-1}$ for all dipoles in the classical model; no radiative decay is included in the quantum model. The solid line is calculated using quantum mechanics and the circles are calculated using our classical method. 61

3-4 (Top) Fraction of energy transferred as a function of time for a donor with a single excited state $\hbar\omega_d = 1.661$ eV and an acceptor with a continuum of 2800 states evenly spaced in the range $\hbar\omega_a = 1.64$ eV to $\hbar\omega_a = 1.68$ eV. The square of the transition dipole moment is 0.35 for the donor. The square of the transition dipole moments for the acceptor are a Lorentzian with maximum of 0.13 at $\hbar\omega_a = 1.66$ eV and width of $\hbar\omega_a = 0.0019$ eV. Parameters: $r = 15$ Å, $\epsilon = \epsilon_0$. The radiative decay rate is $(30\text{ ns})^{-1}$ for all dipoles in the classical model; no radiative decay is included in the quantum model. The solid line is calculated using quantum mechanics and the circles are calculated using our classical method. (Bottom) Imaginary part of the response function for the donor and acceptor. 62

4-1 Rate of population transfer as a function of reorganization energy for a dimer with asymmetry $\Delta = 100\text{ cm}^{-1}$, coupling $J = 20\text{ cm}^{-1}$, ohmic spectral density as in Eq. (4.59) with inverse bath correlation time $\gamma = 53\text{ cm}^{-1}$, and temperature $T = 300$ K. The solid line is calculated by performing a full polaron transform, the crosses are calculated without performing a polaron transform, and the open circles are calculated using the variational technique explained in the text. 94

4-2 Population of donor state as a function of time for a dimer with asymmetry $\Delta = 100$ cm^{-1}, coupling $J = 100$ cm^{-1}, ohmic spectral density as in Eq. (4.59) with inverse bath correlation time $\gamma = 53$ cm^{-1}, and temperature $T = 300$ K. The dynamics are plotted for four different values of the bath reorganization energy λ. The dotted line is computed without performing a polaron transform, while the solid line is computed using the variational polaron transform introduced in the text. The dashed line for $\lambda = 20$ cm^{-1} is computed using a full polaron transform. (The full polaron transform result is not included on the other plots as it yields unphysical results for $\lambda = 2$ cm^{-1} and is identical to the variational result for $\lambda = 100$ cm^{-1} and $\lambda = 500$ cm^{-1}.) 95

4-3 Renormalized electronic coupling, J_p as a function of reorganization energy for a dimer with asymmetry $\Delta = 100$ cm^{-1}, coupling $J = 100$ cm^{-1}, ohmic spectral density as in Eq. (4.59) with inverse bath correlation time $\gamma = 53$ cm^{-1}, and temperature $T = 300$ K. J_p is computed using the variational polaron transformation described in the text. 96

4-4 Population of donor state as a function of time for a dimer coupled to a bath with superohmic spectral density given by Eq. (4.60) with $\eta = 1$. The dynamics are plotted for four different values of the energy splitting Δ and coupling J, as indicated on each figure. The dotted line is computed without performing a polaron transform, the dashed line for is computed using a full polaron transform, and the solid line is computed using the variational polaron transform introduced in the text. Units are such that $\hbar = \omega_c = k_B T = 1$. 98

4-5 Population of donor state as a function of time for a dimer coupled to a bath with superohmic spectral density given by Eq. (4.60) with $\eta = 3$. The dynamics are plotted for four different values of the energy splitting Δ and coupling J, as indicated on each figure. The dotted line is computed without performing a polaron transform, the dashed line for is computed using a full polaron transform, and the solid line is computed using the variational polaron transform introduced in the text. Units are such that $\hbar = \omega_c = k_B T = 1$. 99

5-1 Rate of population transfer as a function of reorganization energy for a dimer with asymmetry $\Delta = 100$ cm^{-1}, coupling $J = 20$ cm^{-1}, ohmic spectral density as in Eq. (5.15) with inverse bath correlation time $\gamma = 100$ cm^{-1}, and temperature $T = 300$ K. The open circles are calculated by the variational minimization described in Chapter 4 while the crosses are calculated using the equilibrium technique in this chapter. 115

5-2 Population of donor state as a function of time for a dimer with splitting $\Delta = 1$ and coupling $J = 3/2$. The system is coupled to a bath with superohmic spectral density given by Eq. (5.16), with $\omega_c = 0.75$. The dynamics are plotted for four different values of the system–bath coupling λ, as indicated on each figure. Units are such that $\hbar = k_B T = 1$. The solid lines are calculated by the variational minimization described in Chapter 4 while the dashed lines are calculated using the equilibrium technique in this chapter. 117

Chapter 1

Introduction

Advances in experimental techniques over the past 10–20 years have enabled a wide range of new experiments in physical chemistry. Many of the novel experiments being performed today probe matter in ways that would previously have been restricted to the realm of thought experiments. In particular, atomic force microscopy has progressed so far into the nanoscale that we are now able to pull on individual molecules and measure their force response [1–6]. Meanwhile, two-dimensional electronic spectroscopy is able to probe electronic excitations as they move coherently from state to state in biological systems [7–10].

These experimental advances provide many opportunities for related advances in theoretical chemistry. New theoretical tools are needed to fully understand the results of these experiments, and to guide the direction of future experiments. In this thesis, I present some new theoretical results that have as a common theme the understanding and interpretation of recent experiments in biophysical chemistry. I now briefly overview the results that will be presented here.

First, I present some results on the Jarzynski equality. The relatively recent Jarzynski equality is a relation between work and free energy for a nonequilibrium system [11] and has found application in the interpretation of biomolecule-pulling experiments [3, 4, 12–14]. There has been some controversy regarding the Jarzynski equality, from whether it is fundamentally correct or even well-defined to whether it can be practically applied. A resolution of these open questions regarding the Jarzyn-

ski equality is important so that experimenters can understand when and whether it can be applied to interpret their experiments. In Chapter 2, I briefly review the Jarzynski equality and examine one particular criticism that has been directed toward it—namely that an ambiguity in the Hamiltonian for time-dependent systems causes the Jarzynski equality to produce arbitrary and unphysical results. In particular, I demonstrate that this particular criticism of the Jarzynski is unfounded and that the Jarzynski equality is indeed fundamentally correct. Much of the work in this chapter was published in Ref. [15].

Next, I present a few recent results on the general topic of coherent resonance energy transfer. One of the most interesting discoveries made with two-dimensional electronic spectroscopy has been the observation of long-lived coherence between protein pigments in photosynthetic complexes [7, 8]. These results have spurred a great deal of interest in the mechanisms of energy transfer in such systems, in particular on the role that quantum coherence plays in the energy-transfer process [16]. In order to answer these questions, it is important to have theories that can predict and explain the dynamics of energy transfer in biologically relevant parameter ranges [17]. It is the development of such theories that is the focus of the remaining chapters.

In Chapter 3, I present a model for coherent resonance energy transfer based on classical electrodynamics. I then show how this model can capture dynamics in the fully coherent regime, in the fully incoherent regime, and in between these two limits. These results show that it is possible to obtain coherent energy transfer dynamics from a classical model. Thus, while biological molecules are certainly fundamentally quantum mechanical, the observation of oscillations in the energy transfer may not be a fundamentally quantum property of the system. Much of the work in this chapter was published in Ref. [18].

In Chapter 4, I turn to a quantum model for energy transfer with the goal of obtaining semiquantitative results for coherent energy transfer. One of the challenges of modeling coherent energy transfer in the biologically relevant regime is that many of the parameters of the system are of approximately the same magnitude. It is thus difficult to find an appropriate perturbative parameter, and most existing perturba-

tive techniques perform well only in limited parameter regimes. In this chapter, I present a variational technique to select an appropriate perturbation and apply the result to calculate the dynamics of resonance energy transfer. This theory is both computationally inexpensive and gives reasonable results over a wide range of parameter values. Much of the work in this chapter forms the second half of a paper currently in press [19].

Finally, in Chapter 5, I continue with the variational polaron transform and briefly explore an alternative method for selecting the optimal transformation. In particular I use exact equilibrium results obtained by a different method as input to the minimization procedure, with the goal of improving the results at a modest increase in computational cost. While the results perform reasonably well at small system–bath interaction, they perform worse than the theory in Chapter 4 at large system–bath interaction. These results are then briefly discussed and explained. As of this writing, the material in this chapter has not yet been submitted for publication.

Bibliography

[1] L. Tskhovrebova, J. Trinick, J. A. Sleep, and R. M. Simmons. Elasticity and unfolding of single molecules of the giant muscle protein titin. *Nature* **387**, 308 (1997).

[2] M. S. Z. Kellermayer, S. B. Smith, H. L. Granzier, and C. Bustamante. Folding–unfolding transitions in single titin molecules characterized with laser tweezers. *Science* **276**, 1112 (1997).

[3] J. Liphardt, S. Dumont, S. B. Smith, I. Tinoco Jr., and C. Bustamante. Equilibrium information from nonequilibrium measurements in an experimental test of Jarzynski's equality. *Science* **296**, 1832 (2002).

[4] D. Collin, F. Ritort, C. Jarzynski, S. B. Smith, I. Tinoco, and C. Bustamante. Verification of the Crooks fluctuation theorem and recovery of RNA folding free energies. *Nature* **437**, 231 (2005).

[5] S. B. Smith, Y. Cui, and C. Bustamante. Overstretching B-DNA: The elastic response of individual double-stranded and single-stranded DNA molecules. *Science* **271**, 795 (1996).

[6] S. Smith, L. Finzi, and C. Bustamante. Direct mechanical measurements of the elasticity of single DNA molecules by using magnetic beads. *Science* **258**, 1122 (1992).

[7] G. S. Engel, T. R. Calhoun, E. L. Read, T.-K. Ahn, T. Mančal, Y.-C. Cheng,

R. E. Blankenship, and G. R. Fleming. Evidence for wavelike energy transfer through quantum coherence in photosynthetic systems. *Nature* **446**, 782 (2007).

[8] H. Lee, Y.-C. Cheng, and G. R. Fleming. Coherence dynamics in photosynthesis: Protein protection of excitonic coherence. *Science* **316**, 1462 (2007).

[9] G. Panitchayangkoon, D. Hayes, K. A. Fransted, J. R. Caram, E. Harel, J. Wen, R. E. Blankenship, and G. S. Engel. Long-lived quantum coherence in photosynthetic complexes at physiological temperature. *Proc. Natl. Acad. Sci. U.S.A.* **107**, 12766 (2010).

[10] E. Collini, C. Y. Wong, K. E. Wilk, P. M. G. Curmi, P. Brumer, and G. D. Scholes. Coherently wired light-harvesting in photosynthetic marine algae at ambient temperature. *Nature* **463**, 644 (2010).

[11] C. Jarzynski. Nonequilibrium equality for free energy differences. *Phys. Rev. Lett.* **78**, 2690 (1997).

[12] N. C. Harris, Y. Song, and C.-H. Kiang. Experimental free energy surface reconstruction from single-molecule force spectroscopy using Jarzynski's equality. *Phys. Rev. Lett.* **99**, 068101 (2007).

[13] W. J. Greenleaf, K. L. Frieda, D. A. N. Foster, M. T. Woodside, and S. M. Block. Direct observation of hierarchical folding in single riboswitch aptamers. *Science* **319**, 630 (2008).

[14] D. K. West, P. D. Olmsted, and E. Paci. Free energy for protein folding from nonequilibrium simulations using the Jarzynski equality. *J. Chem. Phys.* **125**, 204910 (2006).

[15] E. N. Zimanyi and R. J. Silbey. The work-Hamiltonian connection and the usefulness of the Jarzynski equality for free energy calculations. *J. Chem. Phys.* **130**, 171102 (2009).

[16] G. D. Scholes. Quantum-coherent electronic energy transfer: Did nature think of it first? *J. Phys. Chem. Lett.* **1**, 2 (2010).

[17] G. R. Fleming and G. D. Scholes. Physical chemistry: Quantum mechanics for plants. *Nature* **431**, 256 (2004).

[18] E. N. Zimanyi and R. J. Silbey. Unified treatment of coherent and incoherent electronic energy transfer dynamics using classical electrodynamics. *J. Chem. Phys.* **133**, 144107 (2010).

[19] E. N. Zimanyi and R. J. Silbey. Theoretical description of quantum effects in multichromophoric aggregates. *Phil. Trans. Roy. Soc. A* (2012). In press.

Chapter 2

Jarzynski Equality

2.1 Introduction

The free energy difference between two thermodynamic states can be expressed in terms of the work exerted on the system along a reversible path from one state to the other. In particular, if A_S is the Helmholtz free energy of state S, and w is an amount of work performed on the system, then we have at constant temperature and volume

$$A_{S_2} - A_{S_1} = \int_{S_1}^{S_2} dw, \tag{2.1}$$

provided we perform the integration along a reversible path from S_1 to S_2.

We now make two observations about Eq. (2.1):

- Since the integral is along a reversible path, the system is in equilibrium at all times during the integration. As such, the initial state, the final state, and the path are fully defined in terms of thermodynamic quantities and we do not need to consider any microstates of the system in order to compute the integral.

- The existence of Eq. (2.1) depends on the fact that the work performed along a reversible path is a state function; as such, the integral can be performed along *any* reversible path from S_1 to S_2 and will yield the same free energy difference.

Eq. (2.1) provides a method of experimentally determining free energy differences by measuring work, provided one can find an experimentally accessible reversible path between the states of interest.

In 1997, Jarzynski derived another relation between work and free energy that has come to be known as the "Jarzynski equality" [1]. Just as in Eq. (2.1), the Jarzynski equality is an expression for the free energy difference between two equilibrium thermodynamic states. Where the Jarzynski equality differs, however, is that it expresses this free energy difference in terms of the work along an *irreversible* path.

In order to more concretely introduce the Jarzynski equality, we consider a closed system with a Hamiltonian $\mathcal{H}(x, p; \lambda)$, where (x, p) represents a microstate of the system with coordinates x and momenta p, and λ represents an external parameter (or a set of many external parameters). Suppose that we fix $\lambda = \lambda_1$ and allow the system to come to equilibrium at a fixed temperature T, such as by putting it in contact with a heat bath. The system will then be in a well-defined thermodynamic state; there will be a time-invariant phase-space distribution of (x, p) corresponding to this state. We can of course similarly define another state with $\lambda = \lambda_2$, and the free energy difference between these two states is a perfectly well-defined quantity.

Changing λ will in general perform work on the system, and we can then measure the work performed on the system as we change λ according to some protocol. There are of course many ways to change λ from λ_1 to λ_2. We may do so reversibly by making infinitesimal changes in λ and allowing sufficient time for the system to equilibrate between successive changes. The work measured during such a procedure will of course be the reversible work and will equal to the free energy difference between the states with $\lambda = \lambda_1$ and $\lambda = \lambda_2$.

More generally, we may define any arbitrary protocol for changing λ in time, which we write as $\lambda(t)$. Since the system is no longer in equilibrium throughout the process, the work performed on the system is no longer fully defined in terms of

thermodynamic quantities, but depends on the particular microstates through which the system passes. Of course, if we specify the initial microstate of the system and the work protocol $\lambda(t)$, then the further dynamics of the system are fully determined by Hamilton's equations of motion and the work performed on the system is likewise precisely defined.

Usually, however, we do not prepare the system in a particular microstate but rather in a particular thermodynamic state. The initial microstate will be taken from the phase space distribution of that thermodynamic state, and will in general be different for each realization of the process. As a result, even if we define an initial equilibrium state and a work protocol $\lambda(t)$, we will obtain a different value of work each time we perform the experiment and so we speak of a *distribution* of work values. The shape and width of this distribution will of course depend on the particular system and work protocol under consideration.

For macroscopic systems, the work distribution is typically sharp and fluctuations in the work are frequently ignored. Indeed, introductory textbooks often ignore this distribution in work values and instead speak of a single value for the work along an irreversible path. Of course, this approximation is of exactly the same nature as when one speaks of the energy of an ideal gas at a fixed volume and temperature; there is most certainly still a distribution of energies, but it is overwhelmingly improbable that one will observe an energy that deviates significantly from the average.

The Jarzynski equality states that

$$e^{-\beta \Delta G_t} = \langle e^{-\beta W_t} \rangle, \tag{2.2}$$

where $\beta^{-1} = k_B T$, ΔG_t is the free energy between two well-defined thermodynamic states and W_t is the work performed as the external parameters of the system are changed from λ_1 to λ_2 according to some protocol $\lambda(t)$. The free energy difference is between the equilibrium states with $\lambda = \lambda_1$ and $\lambda = \lambda_2$, both at temperature T. The average is over the distribution of work values obtained by repeating the experiment a large number of times, always starting in the equilibrium state with $\lambda = \lambda_1$ and

always using the same work protocol $\lambda(t)$.

The derivation of the Jarzynski equality relies on the fact that the volume of phase space is the same in both the initial and final states. If phase space volume is not conserved, such as in the expansion or compression of a gas, the Jaryznski equality does not apply [2, 3]; in these cases, it is sometimes possible to find an alternate description of the system that does preserve phase space and to which the Jarzynski equality does apply [4].

We note that while one of the reference states for the free energy is the equilibrium state with $\lambda = \lambda_2$, the system is never actually in this state; at the end of the experiment $\lambda = \lambda_2$ but the system will in general be in a nonequilibrium state (though of course could be allowed to relax to equilibrium given a heat bath and sufficient time). In addition, the temperature in the Jarzynski equality is the temperature of the two reference states, and thus also of the initial state in the experiment, but during the experiment the system will not generally be at the same temperature or even have a well-defined temperature. These points have caused some confusion in the literature, and have been carefully explained by Jarzynski [5, 6].

Jarzynski's result has garnered much interest, as it is one of the few exact results in nonequilibrium statistical mechanics. While Jarzynski's initial derivation considered a closed system undergoing Hamiltonian dynamics as described here, the result has been extended to other cases, including systems strongly coupled to a thermal environment and systems undergoing thermalized dynamics [7–10].

There has also been much discussion about the convergence properties of the Jarzynski equality. In particular, while Eq. (2.2) may be exactly correct, the amount of sampling necessary for the work average to converge is an important practical consideration. Indeed, the presence of the exponential of the work in Eq. (2.2) can cause highly improbable paths to make important contributions to the average and thus to the free energy difference [4, 11–14]. For the purposes of this chapter, however, we will be more interested in the fundamental properties of the Jarzynski equality and refer the reader to the literature for discussions of its convergence properties.

In addition to theoretical interest, the Jarzynski equality also suggested another

way of experimentally determining free energies by measuring work, even if the experiment cannot be done reversibly. In particular, single molecule experiments, such as the stretching of a polymer molecule using an atomic force microscope or laser tweezers, have become common in the last decade [15–19]. The goal is often the determination of the free energy surface along some coordinate of the molecular potential energy surface. Hummer and Szabo have derived an extension to the Jarzynski equality that is particularly suited to extracting free energy profiles from molecular pulling experiments [20] and which has been used in the analysis of the aforementioned pulling experiments.

Although there has been some controversy about the Jarzynski equality and related theoretical advances, it is fair to say that their use in interpreting nano-scale single molecule experiments is widespread. Thus any question that they may be fundamentally in error must be carefully examined.

Recently, questions have been raised about the connection between work and changes in the Hamiltonian for a system with a time-dependent Hamiltonian, casting doubt on the applicability of the Jarzynski equality for computing free energy changes. In particular, Vilar and Rubi have claimed that the connection between work and changes in the Hamiltonian breaks down for systems with a time-dependent Hamiltonian and that this causes the Jarzynski equality to give unphysical results [21–25]. Here, we discuss these questions and show that the Jarzynski equality can be usefully applied to determine physically relevant free energy changes.

2.2 Choice of system and environment

Consider a system with Hamiltonian $\mathcal{H}_0(x, p)$, where x represents the coordinates of the system and p the corresponding momenta, and suppose that this system is subject to a time-dependent force $f(t)$ acting along some coordinate $z(x)$. From the perspective of classical mechanics, we have two options for treating the force. We may consider it as an external force not included in the Hamiltonian of the system; in this case, we study the evolution of a system governed by $\mathcal{H}_0(x, p)$ under the effect

of the external force $f(t)$ acting along $z(x)$. Alternatively, we may include the force in the Hamiltonian of the system and study the evolution of a system governed by the time-dependent Hamiltonian $\mathcal{H}(x,p,t) = \mathcal{H}_0(x,p) - z(x)f(t)$.

In the first case, we are considering a time-independent Hamiltonian under the effect of an external force $f(t)$. According to classical mechanics, the differential work done by an external force is equal to the value of the external force times the differential of its conjugate coordinate; in this case yielding fdz. The total work up to time τ is then

$$W(\tau) = \int_{t=0}^{t=\tau} f(t) d\{z[x(t)]\} \tag{2.3}$$

and we have the usual result that the work done on the system equals the change in its energy,

$$\mathcal{H}_0[x(t_2), p(t_2)] - \mathcal{H}_0[x(t_1), p(t_1)] = W(t_2) - W(t_1). \tag{2.4}$$

The free energy change appropriate for this first description of the system is

$$G(z_2) - G(z_1) = -\log\left[\frac{\int dx \delta[z(x) - z_2] e^{-\mathcal{H}_0(x)}}{\int dx \delta[z(x) - z_1] e^{-\mathcal{H}_0(x)}}\right] \tag{2.5}$$

($k_B T = 1$ throughout this chapter). We note that this free energy is a function of the coordinate z and does not depend at all on the external force f.

In the second case, we consider the time-dependent Hamiltonian $\mathcal{H}(x,p,t) = \mathcal{H}_0(x,p) - z(x)f(t)$. In this description of the system, $f(t)$ is an internal force and there should be no expectation that the work done by $f(t)$ equals the change in energy of the system. Here we consider the *thermodynamic work*,

$$W_t(\tau) = \int_0^\tau dt \frac{\partial \mathcal{H}}{\partial t}. \tag{2.6}$$

As the system in not subject to any external forces, Hamilton's equations of motion imply that [26]

$$\frac{d\mathcal{H}}{dt} = \frac{\partial \mathcal{H}}{\partial t}, \tag{2.7}$$

and we immediately see that W_t equals the total change in energy of the system. The

appropriate free energy change to consider for this description of the system is

$$\Delta G_t(\tau) = G_t(\tau) - G_t(0) = -\log\left[\frac{\int dx e^{-\mathcal{H}(x,\tau)}}{\int dx e^{-\mathcal{H}(x,0)}}\right]. \tag{2.8}$$

This free energy depends on the full time-dependent Hamiltonian $H(x,t)$, including the exerted force f. Since $f(t)$ is the only time-dependent term in the Hamiltonian, we could just as well written this free energy as a function of the force f.

We note, as suggested by Vilar and Rubi [21], that this second description of the system is not unique—adding a term $g(t)$ to the Hamiltonian has no effect on the dynamics of the system but changes the values of W_t and ΔG_t.

In considering the change in free energy when a force f is applied to a harmonic spring of force constant k, Vilar and Rubi describe the system according to the first picture and obtain $\Delta G = W = f^2/2k$ while Horowitz and Jarzynski use the second picture and obtain $\Delta G_t = W_t = -f^2/2k$ [22, 23]. Both of these results are correct in their respective descriptions, and mean different things. In particular, Vilar and Rubi are describing the free energy change associated with changing the length of the spring in the absence of an external force; the force is only a tool used to measure the free energy profile of the free spring. Meanwhile, Horowitz and Jarzynski are describing the free energy change of the combined force–spring system as a function of the force. The discrepancy between the definitions of work in these two papers has previously been noted [27].

The Jarzynski equality is framed in the second of our descriptions and expresses a relation between W_t and ΔG_t [1],

$$e^{-\Delta G_t} = \langle e^{-W_t} \rangle. \tag{2.9}$$

The validity of this expression is not in question—only its utility in describing free energy changes in a system. Vilar and Rubi point out that ΔG_t depends on the arbitrary choice of $g(t)$ in the Hamiltonian and leads to arbitrary free energy changes. If all that can be extracted from the Jarzynski equality is this arbitrary ΔG_t, then the Jarzynski equality seems to be of little use. We shall show, however, that this is

not the case.

Peliti has also examined in some detail the effects of adding a term $g(t)$ to the Hamiltonian [27]. He has claimed that such a term is in fact not arbitrary but is unambiguously determined by the particular experimental setup used to manipulate the system; accordingly, he has claimed that one should not be concerned that $g(t)$ shows up in free energy differences. Here, we take a different approach and show that the term $g(t)$ in fact naturally drops out of any physically relevant free energy changes.

2.3 Description of pulling experiment

Consider a single-molecule pulling experiment, for which the Jarzynski equality has frequently been applied [15–18]. In studying the unfolding of a biomolecule, one is often interested in the free energy profile $G(z)$ as a function of end-to-end distance z. We could map the free energy by reversibly pulling the ends of the molecule and measuring the work exerted by the external force as a function of z. This is of course the classic method and corresponds to Vilar and Rubi's analysis of the harmonic spring.

We could also try to get the free energy profile using the Jarzynski equality. Direct application of the Jarzynski equality to yield ΔG_t gives the free energy difference between the free molecule and the molecule with a certain force applied to it. This is not in itself a particularly useful quantity and is not the free energy profile. Hummer and Szabo have, however, shown how to obtain free energy profiles from single-molecule pulling experiments [20].

Consider an unperturbed system described by a Hamiltonian $\mathcal{H}_0(x,p)$. When a time-dependent perturbation is applied along some coordinate $z(x)$, we write the new Hamiltonian as $\mathcal{H}_0(x,p) + \mathcal{H}'(z,t)$. Hummer and Szabo have shown that the unperturbed free energy profile along coordinate z can then be reconstructed as

$$G(z_0) = -\log\langle\delta[z(t) - z_0]e^{-W_t(t)+\mathcal{H}'(z,t)}\rangle, \tag{2.10}$$

where the average is over all trajectories of the system in the presence of the perturbation [20].

We now apply this result to an ideal, deterministic spring and show how the Jarzynski equality can be used to calculate $G(z)$, thereby reconciling the results of Horowitz and Jarzynski with those of Vilar and Rubi. Our model is

$$\mathcal{H}_0(x,p) = p^2/2m + kx^2/2 \tag{2.11}$$

and

$$\mathcal{H}(x,p,t) = \mathcal{H}_0(x,p) - f_0 t x/\tau. \tag{2.12}$$

This Hamiltonian describes an ideal spring under the effect of an external force which increases uniformly from 0 to f_0 over a time $0 < t < \tau$.

Applying Hummer and Szabo's result to our model, we obtain

$$G(z) = -\log\langle \delta[x(\tau) - z] e^{-W_t(\tau) - f_0 x(\tau)} \rangle, \tag{2.13}$$

where we have used the fact that in this case our coordinate of interest $z(x)$ is just x.

The Hamiltonian equations of motion for the system are $\dot{p} = -kx + f_0 t/\tau$ and $\dot{x} = p/m$, and have the solution

$$x(t) = \frac{f_0 t}{m\omega^2 \tau} + x_0 \cos\omega t + \left(\frac{p_0}{m\omega} - \frac{f_0}{m\omega^3 \tau} \right) \sin\omega t, \tag{2.14}$$

where x_0 is the initial position, p_0 is the initial momentum, and $\omega^2 = k/m$. We assume without loss of generality that both $\sin\omega\tau$ and $\cos\omega\tau$ are nonzero; a similar calculation yields the same results for these two special cases.

We perform the average over trajectories in Eq. (2.13) by integrating over (x_0, p_0) weighted by the initial Boltzmann distribution,

$$e^{-G(z)} = \int dx_0 dp_0 \delta[x(\tau) - z] e^{-W_t - f_0 x(\tau)} e^{-H_0(x_0,p_0)}. \tag{2.15}$$

The delta function can be used to eliminate the integral over p_0, yielding

$$e^{-G(z)} = \frac{m\omega}{|\sin \omega t|} \int dx_0 e^{-W_t - f_0 z - H_0(x_0, p_0)} \tag{2.16}$$

where now p_0 is now a function of x_0, defined implicitly according to Eq. (2.14) and the condition $x(\tau) = z$. The factor in front of the integral comes from the coefficient of p_0 in the delta function.

Using the definition of W_t from Eq. (2.6), we find that

$$W_t(\tau) = -\frac{f_0}{\tau} \int_0^\tau x(t) dt, \tag{2.17}$$

which yields upon integration

$$W_t = -\frac{f_0^2}{2m\omega^2} - \frac{f_0 \left[m\omega^2(x_0 + z) - f_0\right] \tan\left(\frac{\omega\tau}{2}\right)}{m\omega^3\tau}. \tag{2.18}$$

We can now calculate the exponent in Eq. (2.16), which after some rearrangement results in

$$-W_t - f_0 z - \mathcal{H}_0(x_0, p_0) = -\frac{1}{2} m\omega^2 z^2 - \frac{1}{2} m\omega^2 \csc^2(\omega\tau) \left(x_0 + \tilde{x}\right)^2, \tag{2.19}$$

where

$$\tilde{x} = \frac{\omega\tau \left(f_0 - m\omega^2 z\right) \cos \omega\tau - f_0 \sin \omega\tau}{m\omega^3\tau}. \tag{2.20}$$

The first term in Eq. (2.19) is independent of x_0 while the second results in a Gaussian integral when put into Eq. (2.16). We then obtain

$$e^{-G(z)} = \sqrt{2\pi m} e^{-\frac{1}{2} m\omega^2 z^2}, \tag{2.21}$$

and thus

$$G(z) = \frac{1}{2} m\omega^2 z^2 - \log \sqrt{2\pi m}. \tag{2.22}$$

The second term in $G(z)$ is independent of z and simply defines the zero of the overall

free energy profile, but does not affect relative free energies. Since the free energy is only defined up to an overall additive constant, we are free to drop this term and obtain

$$G(z) = \frac{1}{2}m\omega^2 z^2 = \frac{1}{2}kz^2. \tag{2.23}$$

This agrees with Vilar and Rubi and is the expected result for the free energy profile of an ideal spring. This result demonstrates that a correct application of the Jarzynski equality does indeed give the correct free energy profile of an ideal spring.

Consider now the effect of adding an arbitrary $g(t)$ to the general Hamiltonian. The effect on ΔG_t is easily seen from Eq. (2.8) to be

$$\Delta G_t^{new}(\tau) = \Delta G_t(\tau) + [g(\tau) - g(0)], \tag{2.24}$$

showing that relative free energies are indeed affected by a term $g(t)$ in the Hamiltonian, as noted earlier in this chapter and by Vilar and Rubi. Since the term $g(t)$ redefines the zero of energy at each point in time, it is expected that $\Delta G_t(\tau)$ will be affected as it is comparing free energies at two different times. Before ascribing a physical interpretation to ΔG_t, it must be corrected by subtracting this arbitrary change in the zero of energy.

We now examine the effect of an arbitrary $g(t)$ on the free energy profile $G(z)$ computed via Jarzynski's equality. We then have the new Hamiltonian and the new work as

$$\mathcal{H}'^{new}(x,t) = \mathcal{H}'(x,t) + g(t) \tag{2.25}$$

and

$$W_t^{new} = W_t + g(\tau) - g(0). \tag{2.26}$$

The free energy profile given by Eq. (2.10) then becomes

$$G^{new}(z_0) = -\log\langle\delta[z(t) - z_0]e^{-W_t + \mathcal{H}'(z,t) + g(0)}\rangle, \tag{2.27}$$

which can be simplified to

$$G^{new}(z_0) = G(z_0) - g(0). \tag{2.28}$$

So adding a time-dependent term $g(t)$ shifts the overall free energy profile $G(z)$ by an additive constant, but has no effect on relative free energies.

We can also express our current arguments in the language of thermodynamics. For a system at constant entropy S and volume V, the thermodynamic potential of interest is the internal energy, $U(S, V)$. If instead of constant volume, the system is held at constant pressure P, it is more convenient to consider the enthalpy $H(S, P)$ obtained by a Legendre transform as $H = U - PV$. In the case of constant temperature rather than constant entropy, one instead considers free energies: the Helmholtz free energy $A(T, V)$ for a system at constant volume and the Gibbs free energy $G(T, P)$ for a system at constant pressure. Each of these free energies is obtained by a Legendre transformation of the corresponding constant entropy potential, $A = U - ST$ and $G = H - ST$ [28].

Here, being interested in a one-dimensional system, we consider length instead of volume and force instead of pressure, but the principles are the same. Indeed, the free energy of Vilar and Rubi, $G_t(f)$, is analogous to a Gibbs free energy while the free energy profile $G(z)$ is analogous to a Helmholtz free energy. The method of Vilar and Rubi is constructed to measure G as a function of position, $G(z)$, while Horowitz and Jarzynski are calculating G_t as a function of f, $G_t(f)$. If the fluctuations in x are small at a given f (i.e., we are in the thermodynamic limit), we can use the Legendre transform relation $G(z) = G_t(f) + fz$ to convert between the two quantities. Jarzynski's equality, however, is usually applied in a regime where fluctuations are important. In this regime, there is not a simple relation between $G_t(f)$ and $G(z)$ but the method of Hummer and Szabo discussed above can be used to reconstruct $G(z)$ from pulling experiments.

2.4 Conclusion

In conclusion, we have reconciled a recent dispute in the literature by carefully showing how different authors were using different definitions of free energy. In particular, we have demonstrated that by properly applying the Jarzynski equality, the textbook result for the free energy profile of a spring is correctly recovered. More generally, we have shown that free energy profiles computed using the Jarzynski equality and the results of Hummer and Szabo do not depend on arbitrary terms in the Hamiltonian. Most importantly, in light of recent doubts, we have reaffirmed the applicability of the Jarzynski equality to the analysis of single-molecule pulling data.

Bibliography

[1] C. Jarzynski. Nonequilibrium equality for free energy differences. *Phys. Rev. Lett.* **78**, 2690 (1997).

[2] J. Sung. Theoretical test of Jarzynski's equality for reversible volume-switching processes of an ideal gas system. *Physical Review E* **76**, 012101 (2007).

[3] J. Sung. Application range of Jarzynski's equation for boundary-switching processes. *Physical Review E* **77**, 042101 (2008). PRE.

[4] S. Pressé and R. Silbey. Ordering of limits in the Jarzynski equality. *J. Chem. Phys.* **124**, 054117 (2006).

[5] C. Jarzynski. Equilibrium free energies from nonequilibrium processes. *Acta Phys. Pol. B* **29**, 1609 (1998).

[6] E. G. D. Cohen and D. Mauzerall. A note on the Jarzynski equality. *J. Stat. Mech.: Theory Exp.* **2004**, P07006 (2004).

[7] C. Jarzynski. Nonequilibrium work theorem for a system strongly coupled to a thermal environment. *J. Stat. Mech.: Theory Exp.* **2004**, P09005 (2004).

[8] M. A. Cuendet. Statistical mechanical derivation of Jarzynski's identity for thermostated non-Hamiltonian dynamics. *Phys. Rev. Lett.* **96**, 120602 (2006).

[9] E. Schöll-Paschinger and C. Dellago. A proof of Jarzynski's nonequilibrium work theorem for dynamical systems that conserve the canonical distribution. *J. Chem. Phys.* **125**, 054105 (2006).

[10] A. Baule, R. M. L. Evans, and P. D. Olmsted. Validation of the Jarzynski relation for a system with strong thermal coupling: An isothermal ideal gas model. *Phys. Rev. E* **74**, 061117 (2006).

[11] S. Pressé and R. J. Silbey. Memory effects on the convergence properties of the Jarzynski equality. *Phys. Rev. E* **74**, 061105 (2006).

[12] C. Jarzynski. Rare events and the convergence of exponentially averaged work values. *Phys. Rev. E* **73**, 046105 (2006).

[13] J. Gore, F. Ritort, and C. Bustamante. From the cover: Bias and error in estimates of equilibrium free-energy differences from nonequilibrium measurements. *Proc. Natl. Acad. Sci. U.S.A.* **100**, 12564 (2003).

[14] A. Suárez, R. Silbey, and I. Oppenheim. Phase transition in the Jarzynski estimator of free energy differences. *Phys. Rev. E* **85**, 051108 (2012).

[15] J. Liphardt, S. Dumont, S. B. Smith, I. Tinoco Jr., and C. Bustamante. Equilibrium information from nonequilibrium measurements in an experimental test of Jarzynski's equality. *Science* **296**, 1832 (2002).

[16] N. C. Harris, Y. Song, and C.-H. Kiang. Experimental free energy surface reconstruction from single-molecule force spectroscopy using Jarzynski's equality. *Phys. Rev. Lett.* **99**, 068101 (2007).

[17] D. Collin, F. Ritort, C. Jarzynski, S. B. Smith, I. Tinoco, and C. Bustamante. Verification of the Crooks fluctuation theorem and recovery of RNA folding free energies. *Nature* **437**, 231 (2005).

[18] W. J. Greenleaf, K. L. Frieda, D. A. N. Foster, M. T. Woodside, and S. M. Block. Direct observation of hierarchical folding in single riboswitch aptamers. *Science* **319**, 630 (2008).

[19] D. K. West, P. D. Olmsted, and E. Paci. Free energy for protein folding from nonequilibrium simulations using the Jarzynski equality. *J. Chem. Phys.* **125**, 204910 (2006).

[20] G. Hummer and A. Szabo. From the cover: Free energy reconstruction from nonequilibrium single-molecule pulling experiments. *Proc. Natl. Acad. Sci. U.S.A.* **98**, 3658 (2001).

[21] J. M. G. Vilar and J. M. Rubi. Failure of the work-Hamiltonian connection for free-energy calculations. *Phys. Rev. Lett.* **100**, 020601 (2008).

[22] J. Horowitz and C. Jarzynski. Comment on "Failure of the work-Hamiltonian connection for free-energy calculations". *Phys. Rev. Lett.* **101**, 098901 (2008).

[23] J. M. G. Vilar and J. M. Rubi. Vilar and Rubi reply. *Phys. Rev. Lett.* **101**, 098902 (2008).

[24] L. Peliti. Comment on "Failure of the work-Hamiltonian connection for free-energy calculations". *Phys. Rev. Lett.* **101**, 098903 (2008).

[25] J. M. G. Vilar and J. M. Rubi. Vilar and Rubi reply. *Phys. Rev. Lett.* **101**, 098904 (2008).

[26] H. Goldstein. *Classical Mechanics* (Addison-Wesley, Reading, MA, 1950), p. 217.

[27] L. Peliti. On the work–Hamiltonian connection in manipulated systems. *J. Stat. Mech.* **2008**, P05002 (2008).

[28] R. J. Silbey, R. A. Alberty, and M. G. Bawendi. *Physical Chemistry*, 4th edition (Wiley, Hoboken, NJ, 2005), pp. 103–108.

Chapter 3

Classical Energy Transfer

3.1 Introduction

Resonance energy transfer (RET), the transfer of electronic energy via nonradiative dipole–dipole coupling, is ubiquitous in chemistry and biology [1–3]. For a system to undergo RET, it must have a donor chromophore and an acceptor chromophore; the donor is initially excited and transfers its energy to the acceptor chromophore. Until recently, most studies involving RET were limited to situations where quantum coherence between the donor and acceptor molecules could be neglected. The theory of RET in this limit was first proposed by Förster, who derived an expression for the rate of energy transfer from a donor to an acceptor molecule [4, 5].

The Förster rate depends on only two quantities: (1) the overlap between the donor emission spectrum and the acceptor absorption spectrum and (2) the distance between the donor and acceptor molecules. As a result, the theory is conceptually simple and depends on a small number of experimentally accessible parameters. While Förster's original derivation was quantum mechanical, it was later shown that the

same result can be obtained from a completely classical picture [6].

Of course, Förster theory cannot be applied in all situations—a good overview of the limitations of this theory and generalizations is found in Ref. [7]. In particular, the incoherent theory of RET relies on Fermi's golden rule, and predicts a constant rate of energy transfer from the donor to the acceptor. Fermi's golden rule will break down if the coupling between the donor and acceptor is too strong, or if the acceptor does not have a high enough density of states. In such situations, the energy of the donor does not transfer unidirectionally to the acceptor, but oscillates coherently between the donor and the acceptor.

Recent experiments on RET in photosynthetic systems have revealed evidence of quantum coherence on picosecond timescales [8–11]. Understanding energy transfer in these systems will require a theory that can account for both quantum coherence and irreversible energy transfer. While some progress has been made in understanding RET in the coherent regime [12–18], none of the theories proposed to date rival the conceptual simplicity of Förster's theory. In particular, all of the available theories of coherent RET depend on a rather detailed knowledge of the environment surrounding the molecules of interest. This is in contrast to Förster's theory, where the environment is only included through its effect on the spectra of the molecules of interest.

A conceptually simple framework for describing coherent RET using only a few experimentally accessible properties of the donor and acceptor molecules would be highly desirable. In light of this, we wish to examine whether it is possible to describe coherent RET using a model that is based on classical electrodynamics. Many properties of condensed phase systems have been accurately described by using classical electrodynamics to treat the interaction between molecules. In particular, classical electrodynamics has been successfully applied to calculate the optical properties of molecular crystals, polymers, and polarizable fluids [19–23]. One can also use a purely classical model to obtain information on the frequency shifts of oscillating molecules due to their interaction [24, 25]. Finally, much of the work leading up to the classical derivation of Förster theory dealt with calculating changes in lifetime of an emitting

dipole when placed near a reflective surface [26].

In these classical models, one generally considers each molecule in the system to have a known linear response to an electric field; upon application of an electric field to the system, each molecule responds to both this external field and to the field due to the resulting polarizations of all other molecules. The result is a set of coupled linear equations for the polarizations of all of the molecules in the system, which are then solved to obtain the overall electric response of the condensed phase.

With respect to energy transfer, classical models have been use to derive Förster theory [6], as well as to study more complicated situations such as energy transfer between microspherical droplets [27]. The classical theory of energy transfer was also extended by the inclusion of higher multipoles and anisotropic media [28].

While classical models have been successfully applied in many situations, to date no such model exists for coherent RET. A typical quantity of interest in coherent RET is the energy of the acceptor molecule as a function of time after an electric field is applied to the donor. The energy of the acceptor molecule depends quadratically on the electric field applied to the donor; a classical theory of RET would then be required to calculate a second-order response function of the system, whereas most classical theories to date have only dealt with linear response functions.

Kryvohuz and Cao have shown, however, that for a harmonic system the classical and quantum response functions are equal to all orders [29]. The systems of interest in coherent RET are not exactly harmonic, however, and thus we cannot expect the quantum and classical response functions to be exactly equal. Nonetheless, if the response of each molecule can be appropriately described by linear response, the system can be approximately replaced by a collection of Drude oscillators with appropriate frequencies. Such a system of Drude oscillators will behave harmonically on timescales where dissipation is negligible, meaning that quantum and classical response functions will be equivalent. The response functions of this system of Drude oscillators will only approximately describe the real quantum system; the replacement of the actual system by a collection of Drude oscillators is an approximation that will not be valid in all circumstances.

Of course, coherent RET is relevant only when the donor and acceptor are strongly coupled; it is not a priori clear that one can replace each molecule with a collection of Drude oscillators in such a situation. Furthermore, it is not obvious whether it will be possible to describe irreversible energy transfer if dissipation is required to be negligible on timescales of interest. These are questions that will need to be answered by any classical theory of coherent RET. Indeed, the preceding considerations do not prove that one can describe coherent RET with a classical theory, but rather provide motivation for why it might be possible to do so. In the following, we will actually develop such a theory and consider a few simple examples to show that it can indeed provide an accurate description of RET in situations of interest.

In section 3.2, we derive a classical theory for RET. In section 3.3, we show how this classical theory can be derived from quantum mechanics. In section 3.4, we present results obtained using our classical theory and compare them to those obtained using other methods. In section 3.5, we summarize our results and give some concluding remarks.

3.2 Classical theory

In the classical derivation of Förster theory, the donor molecule is considered to be an oscillating dipole. This oscillating dipole radiates an electric field which then impinges on the acceptor molecule. The acceptor molecule absorbs energy from the electric field, and the rate of this energy absorption is the rate of energy transfer from the donor to the acceptor [6]. Förster's incoherent theory requires a knowledge of the emission spectrum of the donor in its environment and the absorption spectrum of the acceptor in its environment. Förster theory does not endeavor to calculate either of these spectra, but assumes them to be known, either from experiment or from a separate calculation.

In this paper, we will generalize Förster theory to include coherence between the donor and the acceptor. Förster's theory requires a knowledge of the absorption spectrum of the acceptor, which is proportional to the imaginary part of its complex

polarizability [30]. In order to account for coherence, our theory will require a knowledge of the full complex polarizabilities of the donor and acceptor molecules. In the same spirit as Förster, we assume these to be known either from experiment or from another calculation.

We first consider the effect of an electric field $\mathbf{E}$ on a molecule embedded in a medium of dielectric constant ϵ_0. Within the regime of linear response, the resulting polarization, $\mathbf{p}$, of the molecule will be

$$\mathbf{p}(\omega) = \epsilon_0 \chi(\omega) \mathbf{E}(\omega), \tag{3.1}$$

where $\chi(\omega)$ is the complex polarizability of the molecule. In general, $\chi(\omega)$ will be a tensor, and the polarization of the molecule will depend on its orientation in the perturbing field. In the following, the explicit dependence of the above terms on ω will be omitted except where needed for clarity.

Let us now consider a situation where there are two molecules embedded in the medium, a donor (D) at position $\mathbf{r}_D$ and an acceptor (A) at position $\mathbf{r}_A$. Applying Eq. (3.1) separately to each molecule, we obtain a system of two equations for the polarizations of the two molecules, $\mathbf{p}_D$ and $\mathbf{p}_A$,

$$\begin{cases} \mathbf{p}_D = \epsilon_0 \chi_D \mathbf{E}(\mathbf{r}_D) \\ \mathbf{p}_A = \epsilon_0 \chi_A \mathbf{E}(\mathbf{r}_A). \end{cases} \tag{3.2}$$

The notation $\mathbf{E}(\mathbf{r}_D)$ represents the total electric field at the position of the donor (and similarly for the acceptor). This electric field can be decomposed into an externally applied field, $\mathbf{E}_{\text{ext}}$, and the field due to the presence of the other dipole, $\mathbf{E}_{\text{int}}$,

$$\begin{cases} \mathbf{E}(\mathbf{r}_D) = \mathbf{E}_{\text{ext}}(\mathbf{r}_D) + \mathbf{E}_{\text{int}}(\mathbf{r}_D) \\ \mathbf{E}(\mathbf{r}_A) = \mathbf{E}_{\text{ext}}(\mathbf{r}_A) + \mathbf{E}_{\text{int}}(\mathbf{r}_A). \end{cases} \tag{3.3}$$

In order to calculate the contribution to the field at each molecule due to the presence of the other molecule, we need an expression for the electric field produced by

an oscillating dipole. In general, this is a problem of time-dependent electrodynamics and we must account for the retardation of the field. In particular, McLachlan has examined in detail the effect of retardation on dispersion forces between molecules [31]. Nevertheless, if the size of each dipole and the distance between the dipoles are both much smaller than the wavelength of light at frequencies of interest, it is appropriate to compute the instantaneous dipole as a problem of electrostatics; the details of this approximation are provided in Appendix 3.6.

For configurations relevant to coherent energy transfer, the size of each dipole and the distance between dipoles will each be at most a few nanometers, while the relevant wavelength of light will be of the order of several hundred nanometers [8, 9]. We are thus justified in using the expression from electrostatics for the electric field of a dipole,

$$\mathbf{E}(\mathbf{r}) = \frac{3\hat{\mathbf{n}}(\mathbf{p}\cdot\hat{\mathbf{n}}) - \mathbf{p}}{4\pi\epsilon_0|\mathbf{r}-\mathbf{r}_0|^3}, \tag{3.4}$$

where $\mathbf{r}_0$ is the position of the source dipole and $\hat{\mathbf{n}}$ is the unit vector directed from $\mathbf{r}_0$ to $\mathbf{r}$.

Defining the tensor Φ as

$$\Phi = \frac{3\hat{\mathbf{n}}\hat{\mathbf{n}} - 1}{4\pi\epsilon_0|\mathbf{r}_A-\mathbf{r}_D|^3}, \tag{3.5}$$

where $\hat{\mathbf{n}}$ is the unit vector directed from $\mathbf{r}_D$ to $\mathbf{r}_A$, we can now write the polarization of the two molecules as

$$\begin{cases} \mathbf{p}_D = \epsilon_0\chi_D[\mathbf{E}_{\text{ext}}(\mathbf{r_D}) + \Phi\mathbf{p}_A] \\ \mathbf{p}_A = \epsilon_0\chi_A[\mathbf{E}_{\text{ext}}(\mathbf{r_A}) + \Phi\mathbf{p}_D]. \end{cases} \tag{3.6}$$

The two equations are now closed, and the polarization of each molecule can be found in terms of the applied external fields. In order to simplify the following treatment, we will assume that each molecule is only polarizable along a single axis $\hat{\mathbf{n}}_i$ and that the external field applied to each molecule is along this axis of polarization. As a result, we have $\chi_i = \chi_i\hat{\mathbf{n}}_\mathbf{i}\hat{\mathbf{n}}_\mathbf{i}$, $\mathbf{p}_i = p_i\hat{\mathbf{n}}_i$, and $\mathbf{E}_{\text{ext}}(\mathbf{r_i}) = E_{i,\text{ext}}\hat{\mathbf{n}}_i$.

We can then recast Eq. (3.6) in terms of scalar quantities,

$$\begin{cases} p_D = \epsilon_0 \chi_D [E_{D,\text{ext}} + \phi p_A] \\ p_A = \epsilon_0 \chi_A [E_{A,\text{ext}} + \phi p_D], \end{cases} \tag{3.7}$$

where ϕ is a new scalar coupling between the dipoles and is defined by

$$\phi = \hat{\mathbf{n}}_\mathbf{D} \cdot \Phi \cdot \hat{\mathbf{n}}_\mathbf{A} = \frac{3(\hat{\mathbf{n}} \cdot \hat{\mathbf{n}}_D)(\hat{\mathbf{n}} \cdot \hat{\mathbf{n}}_A) - \hat{\mathbf{n}}_D \cdot \hat{\mathbf{n}}_A}{4\pi\epsilon_0 |\mathbf{r}_A - \mathbf{r}_D|^3}. \tag{3.8}$$

Consistent with our interest in energy transfer, we will suppose that only the donor is irradiated by an external field and study the transfer of energy to the acceptor. Then solving Eq. (3.7) with $E_{D,\text{ext}} = E$ and $E_{A,\text{ext}} = 0$, we obtain

$$p_D(\omega) = \frac{\epsilon_0 E(\omega) \chi_D(\omega)}{1 - \phi^2 \epsilon_0^2 \chi_D(\omega) \chi_A(\omega)} \tag{3.9a}$$

and

$$p_A(\omega) = \frac{\phi \epsilon_0^2 E(\omega) \chi_D(\omega) \chi_A(\omega)}{1 - \phi^2 \epsilon_0^2 \chi_D(\omega) \chi_A(\omega)}. \tag{3.9b}$$

We note that the expressions for $p_D(\omega)$ and $p_A(\omega)$ have poles that are shifted from the poles of the bare response functions $\chi_D(\omega)$ and $\chi_A(\omega)$ by the interaction ϕ.

At this point, we have found the polarization of each molecule in the presence of an external field; as discussed in the introduction, similar results have been obtained in other contexts [19–22]. We now present the main new contribution of our paper, which is to use these polarizations to calculate the rate of energy transfer from the donor to the acceptor. From our current perspective of classical electrodynamics, energy transfer occurs when one of the molecules absorbs energy from the electric field set up by the other molecule.

In order to calculate the rate of energy transfer to the acceptor molecule, we consider the Poynting vector

$$\mathbf{S} = \mathbf{E} \times \mathbf{H}, \tag{3.10}$$

which represents the electrodynamical energy flux; the symbol $\mathbf{H}$ represents the mag-

netic field. In order to consider the rate of energy entering or leaving a volume in space, we compute the divergence of the Poynting vector within the region of the acceptor molecule. Using Maxwell's equations and assuming the absence of free currents or charges, we can write [32]

$$R \equiv -\nabla \cdot \mathbf{S} = \frac{\partial \mathbf{B}}{\partial t} \cdot \mathbf{H} + \frac{\partial \mathbf{D}}{\partial t} \cdot \mathbf{E}, \tag{3.11}$$

where $\mathbf{B}$ is the magnetic induction and $\mathbf{D}$ is the electric displacement.

We then express $\mathbf{D} = \epsilon_0 \mathbf{E} + \mathbf{P}$ and $\mathbf{B} = \mu_0 \mathbf{H}$, where $\mathbf{P}$ is the polarization per unit volume of the acceptor molecule and we have neglected any magnetization of the acceptor molecule, to obtain

$$R = \mu_0 \frac{\partial \mathbf{H}}{\partial t} \cdot \mathbf{H} + \epsilon_0 \frac{\partial \mathbf{E}}{\partial t} \cdot \mathbf{E} + \frac{\partial \mathbf{P}}{\partial t} \cdot \mathbf{E}. \tag{3.12}$$

We can then split R into the part due to the presence of the acceptor, R_a, and the part that would be present in free space, R_0,

$$R = R_0 + R_a, \tag{3.13}$$

where

$$R_0 = \mu_0 \frac{\partial \mathbf{H}}{\partial t} \cdot \mathbf{H} + \epsilon_0 \frac{\partial \mathbf{E}}{\partial t} \cdot \mathbf{E} \tag{3.14}$$

and

$$R_a = \frac{\partial \mathbf{P}}{\partial t} \cdot \mathbf{E}. \tag{3.15}$$

In order to obtain the rate of energy flow to the acceptor we need to integrate R_a over the volume of the acceptor molecule. We assume that the field changes negligibly over the volume of the acceptor molecule, such that only the polarization per unit volume $\mathbf{P}$ needs to be integrated. But the integral of $\mathbf{P}$ over the acceptor molecule simply yields the dipole moment of the acceptor molecule, and we thus have that the

rate of absorption of energy by the acceptor is

$$\dot{Q}_A = E_A(t)\dot{p}_A(t), \tag{3.16}$$

where $E_A(t)$ is the electric field acting on the acceptor at time t and we have used our assumption that the fields and polarizations are along the same axis to replace the vectors with scalars.

Finally, we can use $E_A(t) = \phi p_D(t)$ to write an expression for the energy absorbed by the acceptor as a function of time,

$$\dot{Q}_A(t) = \phi p_D(t)\dot{p}_A(t). \tag{3.17}$$

Of course, Eq. (3.17) depends on the polarizations of the molecules in the time domain while our earlier analysis has produced equations for them in the frequency domain. Transforming Eq. (3.17) into the frequency domain yields

$$\tilde{\dot{Q}}_A(\omega) = -i\phi \int_{-\infty}^{\infty} d\omega' \omega' \tilde{p}_D(\omega - \omega')\tilde{p}_A(\omega'). \tag{3.18}$$

When considering simple models for the response functions, it may be possible to evaluate this convolution analytically and obtain a closed-form expression for $\tilde{Q}_A(\omega)$. In most cases, however, it will be more fruitful to numerically transform $\tilde{p}_D$ and $\tilde{p}_A$ to the time domain so that they can be directly used in Eq. (3.17). We will use this latter approach here.

Before proceeding, however, we will first show how Förster theory can be recovered from Eq. (3.18) in the appropriate limit. First, we rewrite $\tilde{p}_A = \phi\epsilon_0\chi_A\tilde{p}_D$ to obtain

$$\tilde{\dot{Q}}_A(\omega) = -i\phi^2\epsilon_0 \int_{-\infty}^{\infty} d\omega' \omega' \tilde{p}_D(\omega - \omega')\chi_A(\omega')\tilde{p}_D(\omega'). \tag{3.19}$$

In order to compare with the Förster rate, we need to integrate out oscillations in the transfer rate and consider only the constant piece of the rate; this corresponds to taking the $\omega = 0$ component of Eq. (3.19). Using the fact that $\tilde{p}_D(-\omega) = \tilde{p}_D^*(\omega)$, we

obtain

$$\dot{\tilde{Q}}_A(0) = -i\phi^2\epsilon_0 \int_{-\infty}^{\infty} d\omega' \omega' \tilde{p}_D^*(\omega')\chi_A(\omega')\tilde{p}_D(\omega'). \tag{3.20}$$

The symmetry properties of the integrand allows us to rearrange this result as

$$\dot{\tilde{Q}}_A(0) = 2\phi^2\epsilon_0 \int_{0}^{\infty} d\omega\omega\tilde{p}_D(\omega)\chi_A''(\omega)\tilde{p}_D^*(\omega), \tag{3.21}$$

where $\chi_A''(\omega)$ is the imaginary part of $\chi_A(\omega)$ and we have used the fact that $\chi_D(-\omega) = \chi_D^*(\omega)$.

We see that the energy transfer rate can be expressed as the overlap between $\chi_A''(\omega)$ and $\tilde{p}_D(\omega)\tilde{p}_D^*(\omega)$, which is (up to a multiplicative constant) the overlap between the acceptor absorption spectrum and the donor emission spectrum. Furthermore, Eq. (3.21) exactly reproduces the result of Chance et al. for the rate of energy transfer in the incoherent limit [6]. After deriving their result, Chance et al. show that it can be recast into a form identical to that of Förster; the same treatment applies here and the reader is referred to Ref. [6] for details. We note that the present theory predicts the donor emission spectrum to be identical to its absorption spectrum, thereby neglecting any Stokes shift. If the donor emission spectrum is known, it can be used in place of the donor absorption spectrum in the incoherent theory; the result is then identical to Förster theory and also includes the Stokes shift of the donor. A more detailed discussion of donor relaxation is given in section 3.4.

Starting from χ_D and χ_A, we have applied classical electrodynamics to arrive at an expression for the rate of energy transfer between the molecules as a function of time. We have proceeded in the same spirit as Förster and have obtained a theory that logically extends Förster theory to the coherent regime.

3.3 Quantum mechanical theory

We now present a quantum mechanical approach to the problem presented in the last section, with the goal of understanding what approximations are inherent in our classical approach. First, we comment briefly on the correspondence between quantum

and classical results. As discussed in the introduction, the results of Kryvohuz and Cao guarantee that a collection of Drude oscillators will have identical classical and quantum response functions in the absence of dissipation [29].

While the results of Kryvohuz and Cao have motivated our present investigation, we have taken a different approach here. Indeed, our classical theory was not derived by explicitly calculating response functions, which would have involved writing a Hamiltonian and computing several Poisson brackets. Rather, we first calculated the polarizations of the donor and acceptor using their linear response functions; we then used these polarizations to calculate the time-dependent energy transfer rate.

In this section, we will provide a quantum mechanical derivation that proceeds in the same manner as our classical derivation. The goal will be to see what approximations are required to obtain the results of the previous section from a quantum derivation. The results of this section will also allow us to later discuss how a classical model is able to capture features of quantum coherence.

Our system again consists of two molecules. The Hamiltonian for the donor molecule in its environment is H_D, while that for the acceptor molecule in its environment is H_A. We assume that the environments are distinct, with no environmental degree of freedom appearing in both H_D and H_A, which means that

$$[H_D, H_A] = 0. \tag{3.22}$$

The molecules are assumed to interact via a dipole–dipole term,

$$H_{DA} = -\phi \hat{d}_D \hat{d}_A, \tag{3.23}$$

where $\hat{d}_{D(A)}$ represents the dipole operator for the donor (acceptor). In writing the interaction term in this form, we are implicitly including the same assumptions as in the previous section. Namely, we are assuming that each molecule is only polarizable along a single axis; the ϕ that appears here is identical to that in the previous section.

We also allow for an external field $E(t)$ to act on the donor by including the term

$$H_{\text{ext}} = -E(t)\hat{d}_D. \tag{3.24}$$

The total Hamiltonian is then

$$H = H_D + H_A + H_{DA} + H_{\text{ext}}. \tag{3.25}$$

We wish to find the expectation values of $\hat{d}_D(t)$ and $\hat{d}_A(t)$. We shall call these expectation values $p_D(t)$ and $p_A(t)$ in order to clearly distinguish them from their corresponding operators.

We will apply linear response, using $H_0 = H_D + H_A$ as our zeroth-order Hamiltonian and treating $H_{DA} + H_{\text{ext}}$ as a perturbation. All of the linear response functions will be of the general form

$$R_\alpha(t,t') = i \lim_{\eta \to 0} f_\alpha(t,t') e^{\eta(t'-t)} \theta(t-t') \tag{3.26}$$

where $\theta(t)$ is the Heaviside step function and η is a small positive constant. As a result, we will define each response function $R_\alpha(t,t')$ by only giving the corresponding function $f_\alpha(t,t')$.

Applying standard linear response theory, the polarization of the donor is then computed to be

$$p_D(t) = \int_{-\infty}^{\infty} dt' R_D(t,t') E(t') + \phi \int_{-\infty}^{\infty} dt' R_{int}(t,t'), \tag{3.27}$$

where

$$f_D(t,t') = \langle \psi | [\hat{d}_D(t), \hat{d}_D(t')] | \psi \rangle \tag{3.28}$$

and

$$f_{int}(t,t') = \langle \psi | [\hat{d}_D(t), \hat{d}_D(t') \hat{d}_A(t')] | \psi \rangle. \tag{3.29}$$

The time evolution of operators is in the interaction picture of H_0, and $|\psi\rangle$ is the

initial state of the system before the perturbation is turned on.

We recognize $R_D(t,t')$ as the dipole response function of the donor in the medium, χ_D, which we assume to be known or experimentally determined. Turning now to $f_{int}(t,t')$, we can take $\hat{d}_A(t')$ out of the commutator, since operators acting on different molecules commute. This leaves

$$f_{int}(t,t') = \langle\psi|[\hat{d}_D(t), \hat{d}_D(t')]\hat{d}_A(t')|\psi\rangle. \tag{3.30}$$

Since our zeroth-order Hamiltonian does not include any coupling between the two molecules, the ground state of the system can be expressed as a product of a donor state and an acceptor state. The same is true if the initial state $|\psi\rangle$ is taken to be a Boltzmann distribution over the zeroth-order Hamiltonian, since $e^{-\beta(H_D+H_A)} = e^{-\beta H_D}e^{-\beta H_A}$. It is then easy to show that one can factor Eq. (3.30) to obtain

$$f_{int}(t,t') = \langle\psi|[\hat{d}_D(t), \hat{d}_D(t')]|\psi\rangle\langle\psi|\hat{d}_A(t')|\psi\rangle. \tag{3.31}$$

The term $\langle\psi|\hat{d}_A(t')|\psi\rangle$ is equal to zero. The operator $\hat{d}(t')$ is in the Heisenberg picture and evolves only under the zeroth-order Hamiltonian. It is then easy to show that the expectation value of this operator in the ground state will be zero at all times, since the ground state is assumed to have no permanent dipole.

The fact that $f_{int} = 0$ is not surprising, as this term is describing the response of the donor to the polarization of the acceptor. The acceptor itself only becomes polarized due to the field of the donor, so f_{int} is describing a second-order effect and is expected to be zero in linear response.

Rather than proceed to a higher order of perturbation theory, we will attempt to include the interaction between the donor and acceptor in a self-consistent way. In Eq. (3.31), we will replace the zeroth-order polarization of the acceptor, $\langle\psi|\hat{d}_A(t')|\psi\rangle$, with $p_A(t')$, the polarization of the acceptor that includes (at least approximately) the effects of the perturbation. Of course, $p_A(t')$ is not known a priori, but will be solved for self-consistently.

We obtain as a result

$$R_{int}(t,t') = \chi_D(t,t')p_A(t'), \tag{3.32}$$

and the expression for the polarization of the donor then becomes, in Fourier space,

$$\tilde{p}_D(\omega) = \chi_D(\omega)E(\omega) + \phi\chi_D(\omega)\tilde{p}_A(\omega). \tag{3.33}$$

The same method and approximations can be used to find an expression for $\tilde{p}_A$,

$$\tilde{p}_A(\omega) = \phi\chi_A(\omega)\tilde{p}_D(\omega). \tag{3.34}$$

(There would of course be a term depending on the external field had we chosen to allow an external field to act on the acceptor.) We recognize these equations as identical to those derived from classical mechanics in the previous section.

Now we would like to look not only at the expectation value of the dipole moment operator for the two molecules, but also at the energies of the two molecules as a function of time. The method is in principle identical to the one used above to find the dipoles as a function of time—we use linear response with $H_0 = H_D + H_A$ as the zeroth-order Hamiltonian and the rest of the terms as a perturbation.

We would like to calculate the energy of the acceptor as a function of time, given that we already know $p_D(t)$ and $p_A(t)$. Applying linear response, we have

$$Q_A(t) \equiv \langle H_A(t)\rangle = \phi\int_{-\infty}^{\infty} dt' R_\beta(t,t'), \tag{3.35}$$

where

$$f_\beta(t,t') = \langle\psi|[H_A, \hat{d}_D(t')\hat{d}_A(t')]|\psi\rangle. \tag{3.36}$$

We note that H_A is independent of time in the Heisenberg picture since it commutes with the zeroth-order Hamiltonian.

We again factor this expression to obtain

$$f_\beta(t,t') = \langle\psi|[H_A, \hat{d}_A(t')]|\psi\rangle\langle\psi|\hat{d}_D(t')|\psi\rangle. \tag{3.37}$$

This expression as written is equal to zero, for the same reasons as discussed after Eq. (3.31). Again, it is not surprising that a direct application of linear response predicts no energy transfer to the acceptor molecule, since energy transfer is a second-order effect.

Our remedy will be the same as before; we will replace the zeroth-order terms $\langle\psi|[H_A, \hat{d}_A(t')]|\psi\rangle$ and $\langle\psi|\hat{d}_D(t')|\psi\rangle$ with the terms $\dot{p}_A(t')$ and $p_D(t')$ which (approximately) include the effect of the interaction. We then obtain (taking $\eta \to 0$)

$$R_\beta(t,t') = \dot{p}_A(t')p_D(t')\theta(t-t'). \tag{3.38}$$

Our final expression for $Q_A(t)$ is then

$$Q_A(t) = \phi\int_{-\infty}^{t} dt'\dot{p}_A(t')p_D(t'). \tag{3.39}$$

This expression is equivalent to the expression for $\dot{Q}_A(t)$ derived in the previous section using classical electrodynamics.

Now that we have explicitly derived our classical theory from quantum mechanics and seen the inherent approximations, we are in a position to evaluate the circumstances under which our classical theory will be valid.

The most important assumption in our treatment is that of linear response. We assume that both the external field applied to the molecules as well as the fields the molecules exert on one another are weak enough to be correctly treated via linear response.

If we choose the external field to be a delta function in time, $E(\omega) = E$, then the only effect of this field is to prepare the initial state of the system. In an alternate treatment, one might explicitly prescribe the initial state of the system without discussing the external field that brought it to this state; in the present treatment, it is

more convenient to use a delta-function impulse at time $t = 0$ to achieve the same effect.

Consider a simple model system for energy transfer, consisting of four states: the ground state, $|0\rangle$; the state with the donor excited, $|d\rangle$; the state with the acceptor excited, $|a\rangle$; and the state with both donor and acceptor excited, $|da\rangle$. In general, we will consider the system to start in state $|d\rangle$ and we will be interested in the transfer of population to state $|a\rangle$.

Suppose that a delta function pulse at $t = 0$ prepares the system in a state $\alpha|0\rangle + \beta|d\rangle$, after which the system evolves in the absence of an external field. When the external field is not present, the Hamiltonian H of the system will be block diagonal—states $|d\rangle$ and $|a\rangle$ will be coupled but will not interact with states $|0\rangle$ and $|da\rangle$. The populations of states $|d\rangle$ and $|a\rangle$ at a later time t are then

$$P_d(t) = \beta\langle d|e^{iHt}|d\rangle \tag{3.40}$$

and

$$P_a(t) = \beta\langle a|e^{iHt}|d\rangle. \tag{3.41}$$

We notice that $P_d(t)$ and $P_a(t)$ have a very simple linear dependence on β. The dynamics of the energy transfer between $|d\rangle$ and $|a\rangle$ do not depend on β; the only effect of β is to scale the total amount of excitation in the excited states. Thus even if we wish to study energy transfer starting in the pure state $|d\rangle$, it is perfectly acceptable to start in *any* linear superposition $\alpha|0\rangle + \beta|d\rangle$ as long as we scale up the final results by β^{-1}.

Because of the previous argument, we may make the external field E in our model as weak as desired and thus only slightly excite the donor molecule but still obtain dynamics as if the donor molecule were completely excited. Thus if we assume that the external field applied to the donor is a delta function in time, there is no further approximation involved in treating the response of the system to this field by linear response.

We must still consider whether it is appropriate to treat the fields the molecules

exert on one another by linear response. In the next section, we will check the validity of this approximation by comparing our results with those obtained from a more exact quantum mechanical theory.

3.4 Results

In this section, we will apply the theory developed in the previous sections to a few simple but representative cases. In each case, we first construct the complex response functions $\chi_D(\omega)$ and $\chi_A(\omega)$ from the excitation frequencies of the donor and acceptor molecules. The lineshapes are taken to be Lorentzian, such that

$$\chi(\omega) = \frac{e^2}{m_e} \sum_k \frac{2\omega_k p_{0k}^2}{(\omega + \omega_k + i\gamma_k/2)(\omega - \omega_k + i\gamma_k/2)}, \tag{3.42}$$

where e is the charge of the electron, m_e is the mass of the electron, ω_k is the transition frequency from the ground state to state k, γ_k is the radiative decay rate of state k, p_{0k} is the transition dipole moment between the ground state and state k, and the sum is over all excited states of the molecule. The ω_k, γ_k, and p_{0k} are for the molecule in its environment, and thus any effect of the environment is already included in these quantities.

We choose an initial perturbation of the donor that is a delta function in time, $E(\omega) = 1$. The amount of energy absorbed by the donor under this perturbation follows from Eq. (3.16),

$$E_{\text{abs}} = 2\epsilon_0 \int_0^\infty d\omega \omega \chi_D''(\omega). \tag{3.43}$$

Once we have computed the response functions of the molecules, we can use Eq. (3.9) to obtain $p_D(\omega)$ and $p_A(\omega)$. Numerically inverting the Fourier transform of $i\omega p_D(\omega)$ and $p_A(\omega)$ then yields $\dot{p}_D(t)$ and $p_A(t)$. Next, we use Eq. (3.17) to obtain $\dot{Q}_A(t)$ and perform a numerical integration to obtain $Q_A(t)$, the energy absorbed by the acceptor. Finally, we divide $Q_A(t)$ by the total amount of energy that the system absorbs from the initial impulse to obtain the fraction of energy transferred as a function of time.

In order to judge the accuracy of our results, we also compute the fraction of energy transferred as a function of time using quantum mechanics. We include in our calculation all states in which either the donor or the acceptor is singly excited; these are of course the same excited states used to calculate $\chi_D(\omega)$ and $\chi_A(\omega)$ in the classical method. The matrix element of the Hamiltonian between a state where the donor is in its excited state k and a state where the acceptor is in its excited state m is

$$H = \phi p_{d,k} p_{a,m}, \tag{3.44}$$

where ϕ is given by Eq. (3.8), $p_{d,k}$ is the transition dipole moment between the ground state of the donor and its excited state k, and $p_{a,m}$ is the transition dipole moment between the ground state of the acceptor and its excited state m. The matrix element of the Hamiltonian between two states where the same molecule is excited is zero, and the diagonal terms in the Hamiltonian are the energies of the excited states.

For all of the examples considered here, the number of states will be small enough that we can exactly diagonalize the Hamiltonian and thus compute the state of the system at time t as

$$|\psi(t)\rangle = e^{-iHt}|\psi(0)\rangle, \tag{3.45}$$

where $|\psi(0)\rangle$ is the initial state of the system at time $t = 0$. The energy of the acceptor molecule is defined as

$$Q_A(t) = \sum_k \hbar\omega_k P_k(t), \tag{3.46}$$

where P_k and $\hbar\omega_k$ are, respectively, the population and energy of state k, and the sum is over all states where the acceptor is excited. Dividing $Q_A(t)$ by the total energy of the system then yields the fraction of energy transferred as a function of time.

We note that the classical treatment includes a mechanism for excited states to decay to the ground state through the radiative rate γ_k, but that no such mechanism is included in the quantum treatment. In order to compare the two treatments, we can either set $\gamma_k = 0$ in the classical treatment or include radiative decay in the

quantum model, at least in an approximate way. For the examples considered here, however, the timescales of interest are much shorter than the radiative lifetime of the excited states so that radiative decay plays a negligible role in the results. We can thus compare the quantum and classical results without explicitly including radiative decay in our quantum model. While all of our examples will consider a donor molecule with only one excited state, the results are readily generalized to situations where the donor molecule has several excited states.

We first consider the case where the donor and acceptor molecules each have only one excited state. We suppose that the donor has an excited state at $\hbar\omega_d = 1.6600$ eV and the acceptor has an excited state at $\hbar\omega_a = 1.6539$ eV. The molecules are taken to be separated by a distance $r = 9$ Å and the dielectric constant is taken to be that of the vacuum. The transition dipole moment for both molecules is taken to be 1 in atomic units.

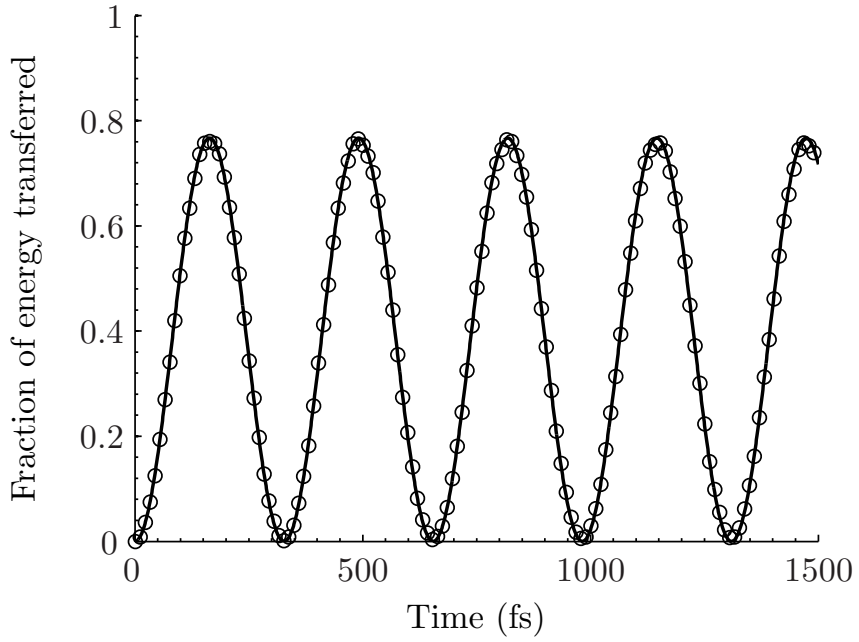

Figure 3-1: Fraction of energy transferred as a function of time for a donor with a single excited state $\hbar\omega_d = 1.6600$ eV and an acceptor with a single excited state $\hbar\omega_a = 1.6539$ eV. Parameters: $r = 9$ Å, $\epsilon = \epsilon_0$, all transition dipole moments are 1 in atomic units. The radiative decay rate is $(80\text{ ns})^{-1}$ for all dipoles in the classical model; no radiative decay is included in the quantum model. The solid line is calculated using quantum mechanics and the circles are calculated using our classical method.

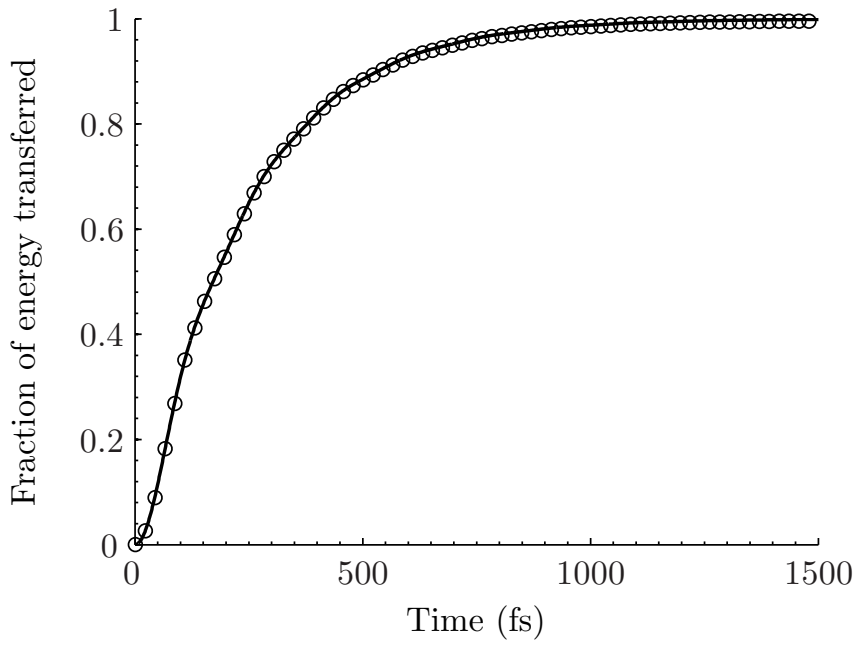

Figure 3-2: Fraction of energy transferred as a function of time for a donor with a single excited state $\hbar\omega_d = 1.66$ eV and an acceptor with a continuum of 75 excited states evenly spaced in the range $\hbar\omega_a = 1.635$ eV to $\hbar\omega_a = 1.685$ eV. The transition dipole moments are 1 for the donor and 0.1 for all acceptor states. Parameters: $r =$ 9 Å, $\epsilon = \epsilon_0$. The radiative decay rate is $(80 \text{ ns})^{-1}$ for all dipoles in the classical model; no radiative decay is included in the quantum model. The solid line is calculated using quantum mechanics and the circles are calculated using our classical method.

The results are given in Fig. 3-1, and show quantitative agreement between the quantum and classical results. In particular, we see that the classical method properly accounts for the quantum coherence between the molecules, correctly predicting both the frequency and amplitude of the energy oscillations.

In our first example, the energy is never permanently transferred to the acceptor molecule. In order to ensure that our model properly accounts for this limit, we will consider a case where the donor is weakly coupled to a quasi-continuum of acceptor states. We suppose that the acceptor molecule has 75 states evenly spaced in the energy range $\hbar\omega = 1.635$ eV to $\hbar\omega = 1.685$ eV, and that each of these states has a transition dipole of 0.01 in atomic units. All other parameters are the same as in our first example. The results are given in Fig. 3-2, and again show quantitative agreement between the quantum and classical results.

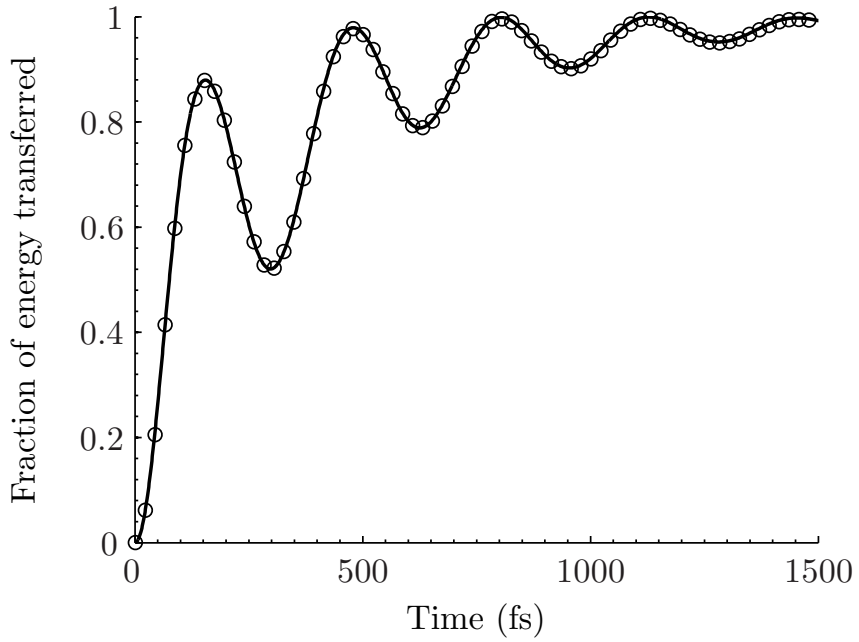

Figure 3-3: Fraction of energy transferred as a function of time for a donor with a single excited state $\hbar\omega_d = 1.66$ eV and an acceptor with a continuum of 75 excited states evenly spaced in the range $\hbar\omega_a = 1.635$ eV to $\hbar\omega_a = 1.685$ eV. The transition dipole moments are 1 for the donor and 0.1 for all acceptor states, except the acceptor state at $\hbar\omega = 1.6539$ eV which has a transition dipole moment of 1. Parameters: $r =$ 9 Å, $\epsilon = \epsilon_0$. The radiative decay rate is $(80 \text{ ns})^{-1}$ for all dipoles in the classical model; no radiative decay is included in the quantum model. The solid line is calculated using quantum mechanics and the circles are calculated using our classical method.

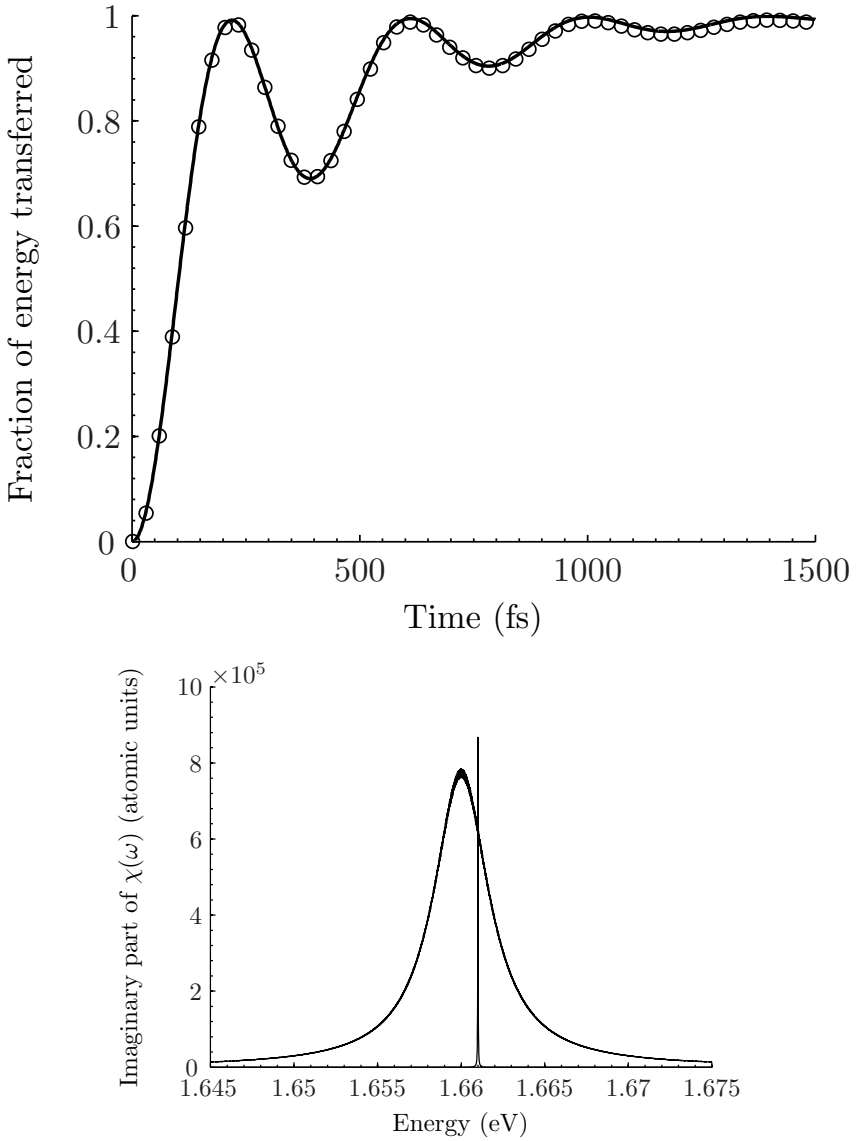

Figure 3-4: (Top) Fraction of energy transferred as a function of time for a donor with a single excited state $\hbar\omega_d = 1.661$ eV and an acceptor with a continuum of 2800 states evenly spaced in the range $\hbar\omega_a = 1.64$ eV to $\hbar\omega_a = 1.68$ eV. The square of the transition dipole moment is 0.35 for the donor. The square of the transition dipole moments for the acceptor are a Lorentzian with maximum of 0.13 at $\hbar\omega_a = 1.66$ eV and width of $\hbar\omega_a = 0.0019$ eV. Parameters: $r = 15$ Å, $\epsilon = \epsilon_0$. The radiative decay rate is $(30\text{ ns})^{-1}$ for all dipoles in the classical model; no radiative decay is included in the quantum model. The solid line is calculated using quantum mechanics and the circles are calculated using our classical method. (Bottom) Imaginary part of the response function for the donor and acceptor.

Next, we consider a hybrid of the first two situations in which the energy oscillates between the two molecules but eventually transfers completely to the acceptor. We do so by taking this last example and making one of the states in the continuum have a transition dipole moment of 1 such that it is strongly coupled to the donor; the state we choose is at $\hbar\omega = 1.6539$ eV. The results are given in Fig. 3-3.

Finally, in Fig. 3-4, we consider a situation where the donor molecule again has only a single excited state, but the absorption spectrum of the acceptor is now a Lorentzian composed of many states. Again, the energy is seen to oscillate at early times but eventually transfers completely to the acceptor.

While the present theory is based on classical electrodynamics, it is clear from the results presented here that it nonetheless captures features of the quantum coherence between the two molecules. In particular, the energy oscillations in Fig. 3-1, which are a signature of quantum coherence between the donor and acceptor, are reproduced identically in the quantum and classical models.

It is not in itself surprising that a classical model can account for back-and-forth energy transfer—two coupled classical springs or two coupled antennae will clearly exhibit such a behavior. In this case, however, the classical model is quantitatively reproducing the quantum results in a regime where quantum coherence is important. It seems then that we are implicitly including the quantum coherence in our classical treatment, though we are of course not calling it as such.

It is well known that classical models can accurately predict the polarizations of molecules in an external field. It is thus not surprising that our model would produce correct values of p_A and p_D. The new and interesting aspect of our theory is that these polarizations can be used to accurately calculate the coherent energy transfer between the molecules, and we now turn to understanding why this is the case.

The time evolution of the energy on molecule 2 can be written exactly as

$$\langle H'_A(t)\rangle = \phi\langle \hat{d}_D(t)\hat{d}'_A(t)\rangle, \tag{3.47}$$

where a prime symbol represents a time derivative. While the classical theory enables

us to compute $\langle \hat{d}_D \rangle$ and $\langle \hat{d}'_A \rangle$, it does not provide us with $\langle \hat{d}_D(t)\hat{d}'_A(t) \rangle$. Indeed, in our classical derivation, we take

$$\dot{Q}_A(t) = \phi p_D(t)\dot{p}_A(t), \tag{3.48}$$

which is only valid if

$$\langle \hat{d}_D(t)\hat{d}'_A(t) \rangle = \langle \hat{d}_D(t) \rangle \langle \hat{d}'_A(t) \rangle. \tag{3.49}$$

Clearly such a factorization is not generally valid for two quantum operators, but let's examine whether it is valid here.

Consider a model system, where the donor and acceptor each have only one excited state. The energy of the donor excited state $|D\rangle$ is $E_0 + \frac{\Delta}{2}$, the energy of the acceptor excited state $|A\rangle$ is $E_0 - \frac{\Delta}{2}$, and the energy of the ground state $|0\rangle$ is 0. As usual, the donor and acceptor are coupled by a term $\phi \hat{d}_D \hat{d}_A$, where

$$\hat{d}_D = q_D(|0\rangle\langle D| + |D\rangle\langle 0|), \tag{3.50}$$

$$\hat{d}_A = q_A(|0\rangle\langle A| + |A\rangle\langle 0|), \tag{3.51}$$

and $q_{D(A)}$ is the transition dipole moment for the donor (acceptor). We assume that $E_0 \gg \phi$ and thus ignore doubly excited states.

We can then solve explicitly,

$$\langle \hat{d}_D(t)\hat{d}'_A(t) \rangle = i(E_0 + \frac{\Delta}{2}) q_D q_A [e^{i\Delta t}\rho_{DA} - e^{-i\Delta t}\rho_{AD}] \tag{3.52}$$

and

$$\langle \hat{d}_D(t) \rangle \langle \hat{d}'_A(t) \rangle = i(E_0 + \frac{\Delta}{2}) q_D q_A [e^{i\Delta t}\rho_{0A}\rho_{D0} - e^{-i\Delta t}\rho_{0D}\rho_{A0}], \tag{3.53}$$

where the ρ is the density matrix for the system in the interaction picture (using $\phi \hat{d}_D \hat{d}_A$ as the perturbation). We have assumed that $E_0 \gg \Delta$ and integrated out oscillations on timescales of E_0^{-1}.

The key feature of this result is that $\langle \hat{d}_D(t)\hat{d}'_A(t) \rangle$ depends on ρ_{DA}, while $\langle \hat{d}_D(t) \rangle \langle \hat{d}'_A(t) \rangle$ depends on ρ_{0D} and ρ_{0A}. The first of these is expected, as it means that rate of energy

transfer between $|D\rangle$ and $|A\rangle$ depends on the coherence between $|D\rangle$ and $|A\rangle$. The second is also expected, since it means that the polarization of the donor depends on the coherence between the ground state and the excited donor state (and similarly for the acceptor).

While ρ_{0D} and ρ_{0A} are coherences, they can be interpreted classically as the polarizations of the two molecules. The coherence ρ_{DA} does not, however, have a direct classical interpretation. For a pure state, however, the idempotency of the density matrix requires that $\rho_{DA} = \rho_{0A}\rho_{D0}/\rho_{00}$; Eqs. (3.52) and (3.53) then become equivalent. Thus as long as the system remains in a pure state, the two sides of Eq. (3.49) are indeed equivalent and we can compute the energy transfer rate knowing only the classical polarizations of the two molecules.

While our example here is a simple system where the donor and acceptor each have only one excited state, the same principles apply when each molecule has many excited states, and the factorization in Eq. (3.49) is again valid. We note that we have assumed that $E_0 \gg \Delta$ and $E_0 \gg \phi$, meaning that the average energy of the excited state manifold is much larger than both the energy splittings between excited states and the couplings between excited states; this is the case for all examples considered here. We have also assumed that the system remains in a pure state, which will be the case as long as we include all relevant states in our quantum description.

For systems where our classical treatment is valid, the energy transfer proceeds just as with classical antennae. While an appropriate quantum treatment would certainly correctly predict the energy transfer dynamics, what we have shown here is that such systems can also be described by classical mechanics. This is not to say that the systems are not quantum mechanical, but rather that the coherent energy transfer dynamics can also be described by a classical model.

Finally, we point out one aspect of the problem that is not included in the present theory. Our method of treating the bath has been to include it as part of the system, and to work in terms of eigenstates of the combined system–bath Hamiltonian. This means that once we excite the donor molecule to an excited state of the donor–bath system, there is no mechanism in our theory for population to nonradiatively transfer

to another excited state of the donor–bath system. The initial pulse may populate several excited states of the donor–bath Hamiltonian, but once these excited states are populated they do not transfer energy among themselves. We are in essence assuming that the Stokes shift for the donor molecule is small on timescales of interest—in our model, the energy absorbed into a given excited state must necessarily be emitted from the same state. This approximation is a direct result of our using linear response, as a perturbation at one frequency can only cause a response at that same frequency.

In reality, of course, the situation is more complicated. Immediately after the initial excitation pulse, the excited state populations of the donor molecule will correspond to its absorption spectrum. The excited states will then transfer energy among themselves until the excited state populations correspond to the emission spectrum. While this energy transfer is happening, the excited state populations correspond to neither the absorption nor the emission spectrum. Förster's theory for incoherent RET uses the emission spectrum for the donor, thereby assuming that the donor molecule has completely relaxed to its emitting state before any energy transfer occurs; this is generally a good approximation in the weak-coupling limit where Förster theory is valid. In the present work, we make the opposite assumption, and ignore any internal relaxation of the donor molecule. Our approximation will be good as long as we are looking at energy transfer on timescales faster than the internal relaxation of the donor molecule. An alternative would be to modify the donor response function such that the excitation pulse directly excites the donor to its emitting state; this method would be equivalent to assuming instantaneous relaxation as in Förster theory. The issue of donor relaxation does not arise in the examples considered here, as the donor molecule has only one excited state and there is thus no way for the donor to nonradiatively relax from one excited state to another.

Förster theory has been generalized to include the time-dependence of the donor emission spectrum [33, 34]. It may be possible to apply a similar approach to the present problem, by allowing the response functions of each molecule to depend on time. Of course, in order to calculate how the response function of each molecule evolves in time, one would likely need detailed information about the bath of the

molecules. One of the attractive features of our present theory is that such a detailed knowledge of the bath is not required—only the experimentally determined χ_D and χ_A are needed. An alternative might be to use experimentally measured information on the time-dependent Stokes shift of the separated donor and acceptor molecules as an input to the theory; this approach would be in keeping with the spirit of the present theory, whereby the bath is not included explicitly but only through its effect on measurable properties.

3.5 Conclusion

We have presented a classical theory for understanding RET in the coherent limit that is both intuitively simple and depends on a small number of experimentally accessible parameters. In particular, our results only require knowledge of the complex polarizabilities of the molecules and the distance between them; the environment is included only through its effect on the polarizabilities. As a result, our theory naturally follows in the same spirit as Förster theory. By applying our theory in situations of interest for RET, we have shown that quantitative agreement with quantum mechanics is obtained. We have explained how our theory, while being classical, can nonetheless quantitatively reproduce energy oscillations in a regime where quantum coherence is important.

Given the recent interest in the role that quantum mechanics plays in coherent RET in biological systems, we find it particularly interesting that a classical model can correctly predict energy transfer dynamics in the coherent regime. Of course, it is clear that the photosynthetic complexes are inherently quantum mechanical in the sense that they obey the laws of quantum mechanics and are able to be described by quantum models. The relevant question is whether their efficient energy transfer relies on the quantum nature of the system, and in particular whether a classical theory could produce similar results. The results here suggest that, at least for the simple models considered here, one can think of coherent energy transfer in terms of interacting antennae that exchange energy as they oscillate in and out of phase. Of

course, as emphasized earlier, a quantum theory may be required in order to understand the internal structure of each antenna; notheless, their interaction is governed by a classical mechanism.

Our classical theory has made certain assumptions about the system, the most important being (1) that the interaction between the molecules is weak enough to be treated via linear response, (2) that the environments of the molecules are uncorrelated, and (3) that the timescale of interest for energy transfer is much faster than the timescale for internal relaxation of each molecule. While there will certainly be situations in which these assumptions fail and a more detailed model is needed, for situations within its limits of validity our classical model provides a simple and intuitive way of calculating energy transfer rates. Furthermore, the examples presented here have shown that our model is indeed valid for many physically realistic situations. It would nonetheless be interesting to examine in the future whether it is possible to relax the above assumptions while still retaining the simplicity and intuitive appeal of our model.

3.6 Appendix—Static Approximation

We use the general expression for the field radiated by a system with time-dependent charge density $\rho(\mathbf{r}, t)$,

$$\mathbf{E}(\mathbf{r}, t) = \frac{1}{4\pi\epsilon_0} \int \left[\frac{\rho(\mathbf{r}', t_r)}{R^2} \hat{\mathbf{R}} + \frac{\dot{\rho}(\mathbf{r}', t_r)}{cR} \hat{\mathbf{R}} - \frac{\dot{\mathbf{J}}(\mathbf{r}', t_r)}{c^2 R} \right] d\mathbf{r}', \tag{3.54}$$

where $\mathbf{R} = \mathbf{r} - \mathbf{r}'$ and $t_r = t - R/c$ [35].

Now $\dot{\rho} \sim \omega\rho$, where ω is the frequency of oscillation of the dipole. So the second term is of order $R\omega/c = R/\lambda$, where λ is the wavelength of light at frequency ω. In the third term, we can write $\mathbf{J} = \rho\mathbf{v}$ where $\mathbf{v}$ is the velocity of the charge in the dipole; then $\dot{\mathbf{J}} = \dot{\rho}\mathbf{v} + \rho\dot{\mathbf{v}}$. If a is the spatial size of the dipole, then $v \sim \omega a$ and

$\dot{v} \sim \omega^2 a$; then $\dot{\mathbf{J}} \sim \rho\omega^2 a$. So the third term is of order $Ra\omega^2/c^2 = Ra/\lambda^2$. Finally,

$$\rho(\mathbf{r}', t - R/c) \approx \rho(\mathbf{r}', t) - \frac{R}{c}\dot{\rho}(\mathbf{r}', t), \tag{3.55}$$

so to order R/λ we can also ignore the ignore the retardation in the first term.

In the cases we will consider, the λ will be a few hundred nanometers, while a and R will be at most 1 or 2 nm. As a result, we can keep only the first term in the above expression and ignore the retardation. We are then left with

$$\mathbf{E}(\mathbf{r}, t) = \frac{\hat{\mathbf{R}}}{4\pi\epsilon_0} \int \frac{\rho(\mathbf{r}', t_r)}{R^2} d\mathbf{r}'. \tag{3.56}$$

This is just the instantaneous field produced by the static charge distribution $\rho(\mathbf{r})$.

Bibliography

[1] P. G. Wu and L. Brand. Resonance energy transfer: Methods and applications. *Analytical Biochemistry* **218**, 1 (1994).

[2] G. D. Scholes. Long-range resonance energy transfer in molecular systems. *Annu. Rev. Phys. Chem.* **54**, 57 (2003).

[3] D. W. Piston and G.-J. Kremers. Fluorescent protein FRET: the good, the bad and the ugly. *Trends Biochem. Sci.* **32**, 407 (2007).

[4] T. Förster. Delocalized excitation and excitation transfer. In *Modern Quantum Chemistry*, O. Sinanoğlu, Ed. (Academic, New York, 1965), pp. 93–137.

[5] T. Förster. Transfer mechanisms of electronic excitation. *Discuss. Faraday Soc.* **27**, 7 (1959).

[6] R. R. Chance, A. Prock, and R. Silbey. Comments on the classical theory of energy transfer. *J. Chem. Phys.* **62**, 2245 (1975).

[7] D. Beljonne, C. Curutchet, G. D. Scholes, and R. J. Silbey. Beyond Förster resonance energy transfer in biological and nanoscale systems. *J. Phys. Chem. B* **113**, 6583 (2009).

[8] G. S. Engel, T. R. Calhoun, E. L. Read, T.-K. Ahn, T. Mančal, Y.-C. Cheng, R. E. Blankenship, and G. R. Fleming. Evidence for wavelike energy transfer through quantum coherence in photosynthetic systems. *Nature* **446**, 782 (2007).

[9] H. Lee, Y.-C. Cheng, and G. R. Fleming. Coherence dynamics in photosynthesis: Protein protection of excitonic coherence. *Science* **316**, 1462 (2007).

[10] G. Panitchayangkoon, D. Hayes, K. A. Fransted, J. R. Caram, E. Harel, J. Wen, R. E. Blankenship, and G. S. Engel. Long-lived quantum coherence in photosynthetic complexes at physiological temperature. *Proc. Natl. Acad. Sci. U.S.A.* **107**, 12766 (2010).

[11] E. Collini, C. Y. Wong, K. E. Wilk, P. M. G. Curmi, P. Brumer, and G. D. Scholes. Coherently wired light-harvesting in photosynthetic marine algae at ambient temperature. *Nature* **463**, 644 (2010).

[12] M. Yang and G. R. Fleming. Influence of phonons on exciton transfer dynamics: comparison of the Redfield, Förster, and modified Redfield equations. *Chem. Phys.* **282**, 163 (2002).

[13] S. Jang, Y.-C. Cheng, D. R. Reichman, and J. D. Eaves. Theory of coherent resonance energy transfer. *J. Chem. Phys.* **129**, 101104 (2008).

[14] S. Jang. Theory of coherent resonance energy transfer for coherent initial condition. *J. Chem. Phys.* **131**, 164101 (2009).

[15] A. Ishizaki and G. R. Fleming. Unified treatment of quantum coherent and incoherent hopping dynamics in electronic energy transfer: Reduced hierarchy equation approach. *J. Chem. Phys.* **130**, 234111 (2009).

[16] M. Mohseni, P. Rebentrost, S. Lloyd, and A. Aspuru-Guzik. Environment-assisted quantum walks in photosynthetic energy transfer. *J. Chem. Phys.* **129**, 174106 (2008).

[17] P. Rebentrost, M. Mohseni, I. Kassal, S. Lloyd, and A. Aspuru-Guzik. Environment-assisted quantum transport. *New J. Phys.* **11**, 033003 (2009).

[18] V. I. Novoderezhkin, M. A. Palacios, H. van Amerongen, and R. van Grondelle. Energy-transfer dynamics in the LHCII complex of higher plants: Modified Redfield approach. *J. Phys. Chem. B* **108**, 10363 (2004).

[19] G. D. Mahan. Optical properties of molecular crystals. In *Electronic structure of polymers and molecular crystals*, J.-M. André and J. Ladik, Eds. (Plenum, New York, 1975), pp. 79–157.

[20] H. DeVoe. Optical properties of molecular aggregates. I. Classical model of electronic absorption and refraction. *J. Chem. Phys.* **41**, 393 (1964).

[21] H. DeVoe. Optical properties of molecular aggregates. II. Classical theory of the refraction, absorption, and optical activity of solutions and crystals. *J. Chem. Phys.* **43**, 3199 (1965).

[22] J. Cao and B. J. Berne. Theory and simulation of polar and nonpolar polarizable fluids. *J. Chem. Phys.* **99**, 6998 (1993).

[23] J. Cao and B. J. Berne. Theory of polarizable liquid crystals: Optical birefringence. *J. Chem. Phys.* **99**, 2213 (1993).

[24] V. L. Lyuboshitz. Scattering of electromagnetic waves by a system of dipole centers. *Sov. Phys. JETP* **25**, 612 (1967).

[25] V. L. Lyuboshitz. Resonance interaction between two identical dipole emitters. *Sov. Phys. JETP* **26**, 937 (1968).

[26] R. R. Chance, A. Prock, and R. Silbey. Decay of an emitting dipole between two parallel mirrors. *J. Chem. Phys.* **62**, 771 (1975).

[27] A. C. Pineda and D. Ronis. Classical model for energy transfer in microspherical droplets. *Phys. Rev. E* **52**, 5178 (1995).

[28] R. R. Chance, A. Prock, and R. Silbey. Comments on the classical theory of energy transfer. II. Extension to higher multipoles and anisotropic media. *J. Chem. Phys.* **65**, 2527 (1976).

[29] M. Kryvohuz and J. Cao. Quantum-classical correspondence in response theory. *Phys. Rev. Lett.* **95**, 180405 (2005).

[30] J. D. Jackson. *Classical Electrodynamics*, 3rd edition (Wiley, New York, 1999), pp. 309–316.

[31] A. D. McLachlan. Retarded dispersion forces between molecules. *Proc. R. Soc. London A* **271**, 387 (1963).

[32] L. D. Landau and E. M. Lifshitz. *Electrodynamics of Continuous Media* (Pergamon Press, Oxford, 1960), pp. 253–255.

[33] S. Mukamel and V. Rupasov. Energy transfer, spectral diffusion, and fluorescence of molecular aggregates: Brownian oscillator analysis. *Chem. Phys. Lett.* **242**, 17 (1995).

[34] S. Jang, Y. Jung, and R. J. Silbey. Nonequilibrium generalization of Förster–Dexter theory for excitation energy transfer. *Chem. Phys.* **275**, 319 (2002).

[35] D. J. Griffiths. *Introduction to Electrodynamics*, 3rd edition (Prentice Hall, Upper Saddle River, N.J., 1999), p. 427.

Chapter 4

Variational polaron transform

4.1 Introduction

While the last chapter developed a classical theory able to explain coherent resonant energy transfer, at least in simple cases, here we turn our attention to a quantum theory of coherent energy transfer. There is of course a large body of work in the literature on the question of understanding energy transfer between electronic states, which will be briefly reviewed in this section as we introduce the necessary ideas to explain the new contribution of this chapter. For the purposes of this chapter, we will consider a two-state system, however the results are not fundamentally limited to systems with only two electronic states.

To be concrete, we consider a two-state system with Hamiltonian

$$H = \begin{pmatrix} \frac{\Delta_0}{2} & J \\ J & -\frac{\Delta_0}{2} \end{pmatrix}, \tag{4.1}$$

where Δ_0 and J are real parameters and the matrix is written in the basis of two electronic states $|1\rangle$ and $|2\rangle$, which are the electronic states between which energy transfer occurs. These two states have an energy splitting Δ_0 and an interaction matrix element J.

The dynamics such a two-state system in the absence of an environment are of

course trivially solvable; the energy transfers back and forth between the two states forever. Such a solution necessarily does not capture dissipation or eventual localization of the energy on one site or the other, features that are present in the real systems that we intend to model. Indeed, it is the interaction between the system and the environment that allows a rich range of dynamics to occur, and also that makes the problem difficult.

In order to include environmental effects on the dynamics of a quantum system, one need not explicitly include the environment. Instead, one could suppose that the parameters of the Hamiltonian fluctuate randomly as a result of the evolution of the (unknown) environment. This stochastic approach to treating environmental effects was pioneered by Kubo in his study of magnetic resonance lineshapes [1, 2].

Haken, Strobl, and Reineker have developed a theory for energy transfer by treating the energy of each site as a stochastic variable [3, 4]. By assuming the fluctuations on each site to be Gaussian and Markovian, and the fluctuations on different sites to be uncorrelated, they were able to arrive at an exactly solvable model that nonetheless captures many of the qualitative features of energy transfer. More recently, the model of Haken et al. has been to include fluctuations in the off-diagonal matrix elements as well as correlated fluctuations [5].

While the technique of using a stochastic Hamiltonian can provide insightful results, the parameters of the stochastic process generally remain phenomenological parameters of the model. One can more directly consider the influence of the environment by including it in the quantum Hamiltonian; this of course requires an explicit model for the environment.

The environment is, by definition, all of the degrees of freedom that we have ignored in writing down the system Hamiltonian. Since the system Hamiltonian considers only electronic excitations, the environment must include rotational and vibrational modes, both of the molecule containing the electronic excitations and of surrounding molecules. Typically, one invokes the Born–Oppenheimer approximation to decouple the fast electronic degrees of freedom from the slower rotational and vibrational degrees of freedom; the electronic state provides a potential surface on

which the nuclei evolve. Sufficiently near the minimum, the potential surface can be taken as quadratic; by expanding the surface around the minimum one obtains a description of the environment in terms of a collection of normal modes.

In the case of two electronic states, there will be two potential surfaces and in general a different minimum for each surface. We can expand the potential surface around the average of the two minima, and if we assume that the two minima are reasonably close together a quadratic expansion should still suffice. Of course here we are not expanding around a minimum of either potential surface so there will generally be a linear exciton–phonon coupling term.

The model we have just outlined is expressed by the spin–boson Hamiltonian:

$$H = \begin{pmatrix} H_B + \frac{\Delta_0}{2} + B_1 & J \\ J & H_B - \frac{\Delta_0}{2} + B_2 \end{pmatrix}, \tag{4.2}$$

where

$$H_B = \sum_j \hbar\omega_j \left(b_j^\dagger b_j + \frac{1}{2} \right), \tag{4.3}$$

$$B_1 = \sum_j \hbar\omega_j g_{1j} (b_j^\dagger + b_j), \tag{4.4}$$

and similarly for B_2. $b_j^\dagger$ and b_j are, respectively, phonon creation and annihilation operators, while g_{1j}, g_{2j}, and ω_j are real numbers. The term H_B describes the harmonic modes of the environment, while B_1 and B_2 describe the coupling between the environment and electronic states 1 and 2, respectively.

We now make several remarks about this Hamiltonian. First, the assumption of linear exciton–phonon coupling will break down if there are environmental modes that couple strongly to the electronic subsystem. One could go to higher order and consider quadratic exciton–phonon coupling as has been done in a different context [6]. If there are a small number of strongly coupled bath modes, one could also choose to treat them explicitly as part of the system Hamiltonian. We shall limit ourselves to linear coupling as there is still a rich range of dynamics to be studied for this case.

The quantities g_{1j}, g_{2j}, and ω_j will often enter our equations in the combination

$$\eta_{1(2)}(\omega) = \sum_j \omega_j^2 g_{1(2)j}^2 \delta(\omega - \omega_j), \tag{4.5}$$

called the *spectral density* of the phonon modes. We are often interested in the behavior of $\eta(\omega)$ at small omega,

$$\eta(\omega) \sim \omega^p \qquad \omega \to 0. \tag{4.6}$$

The spectral density is called *ohmic* when $p = 1$, *subohmic* when $p < 1$, and *super-ohmic* when $p > 1$.

Of course, while we have written down a Hamiltonian in terms of microscopic properties of the system and its environment, the actual determination of the appropriate parameters remains a nontrivial problem. This is in contrast to Förster theory, which is expressed in terms of simple and experimentally accessible quantities—the emission spectrum of the donor, the absorption spectrum of the acceptor, and the donor–acceptor distance. Nonetheless, progress has been made in determining the appropriate parameters for several systems of interest [7–9].

We will generally be interested in the evolution of the electronic excitation as a function of time; while the environment plays in important role in these dynamics, one is not usually interested in the actual state of the environment but only in the state of the system. Instead of computing the entire density matrix of the system, ρ, we shall instead focus on the reduced density matrix of the system, obtained by tracing over the degrees of freedom of the environment, $\rho^S = \mathrm{Tr}_B \rho$.

The Hamiltonian in Eq. (4.2) cannot be exactly diagonalized, and it is impossible to exactly solve for the dynamics of the reduced density matrix except in certain limiting cases. Leggett et al. have been able to obtain exact results for some limited parameter regions and approximate results in other cases through their *non-interacting blip approximation* [10]. In the case of degenerate electronic states, it is possible to formally diagonalize the Hamiltonian by applying a Fulton–Gouterman

transformation, however the results are of little practical use for computing dynamics unless approximations are made [11–13]. Finally, Ishizaki and Fleming have recently developed technique using hierarchical equations that is able to obtain exact results in the case of ohmic spectral density [14]. In addition to the limitation of ohmic spectral density, their method also assumes that the bath modes coupling the two sites are uncorrelated and is also very computationally expensive. There is some evidence that correlated fluctuations may play an important role in excitation energy transfer in biological systems[15, 16].

Beyond these few exact cases, we will need to rely on approximate equations for the reduced density matrix. In particular, we will use a perturbative technique in order to obtain approximate results at modest computational cost. Obtaining a perturbative solution for the reduced density matrix generally follows the prescription: (1) partition the Hamiltonian into a zeroth-order part and a perturbation; (2) obtain an expansion for reduced the density matrix in powers of the perturbation, usually in the form of a *quantum master equation*. The accuracy of a technique of course depends on both of these steps; one can improve the accuracy of a method by either choosing a better density matrix expansion or by choosing a better partitioning of the Hamiltonian.

4.2 Perturbations

In order to approximately solve for the dynamics generated by Eq. (4.2), we now examine perturbative techniques that can be used. If the system–bath coupling were absent ($g_{1k} = g_{2k} = 0$), then the dynamics would trivially solvable. This suggests dividing the Hamiltonian into an exactly solvable zeroth-order part,

$$H_0 = \begin{pmatrix} H_B + \frac{\Delta_0}{2} & J \\ J & H_B - \frac{\Delta_0}{2} \end{pmatrix}, \tag{4.7}$$

and a perturbation

$$H_1 = \begin{pmatrix} B_1 & 0 \\ 0 & B_2 \end{pmatrix}. \tag{4.8}$$

This perturbation is very popular when the environment has only a weak influence on the system, and has the advantage of fully including the donor–acceptor matrix element in the zeroth-order term. It was used by Redfield to explain relaxation in spin systems [17] and has also been widely applied to study energy transfer [18, 19]. Of course, by the nature of the perturbation, it will break down once the system–bath coupling becomes large compared to other parameters in the system; this point was recently emphasized by Ishizaki and Fleming [20].

For systems with strong coupling between electronic and vibrational degrees of freedom, one can apply a *polaron transform* to the system and obtain a description of the system in a new basis:

$$\tilde{H} = e^{G_1+G_2} H e^{-G_1-G_2}, \tag{4.9}$$

where

$$G_k = \sum_j g_{kj}(b_j^\dagger - b_j)|k\rangle\langle k|, \tag{4.10}$$

for $k = 1, 2$.

The resulting Hamiltonian is

$$\tilde{H} = \begin{pmatrix} H_B + \frac{\Delta}{2} - E_{p1} & Je^{G_1}e^{-G_2} \\ Je^{G_2}e^{-G_1} & H_B - \frac{\Delta}{2} - E_{p2} \end{pmatrix}, \tag{4.11}$$

and

$$E_{pk} = \hbar \sum_j g_{kj}^2 \omega_j \tag{4.12}$$

is called the *polaron shift* of state k.

Recalling our earlier description of the environment, the effect of this transformation is to expand the nuclear potential surface for each electronic state around its respective minimum. Since the expansion is always around a minimum, there are no

linear exciton–phonon coupling terms in the Hamiltonian. Of course, by expanding around a different point for each electronic state, the basis states with which we describe the bath depend on which electronic state we are in. As a result, the site–site coupling is no longer simply J but now also contains factors relating to the overlap between basis states.

In the trivial case of non-interacting molecules, $J = 0$, the Hamiltonian has been exactly diagonalized. In the general case, the off-diagonal terms $Je^{G_1}e^{-G_2}$ (and its complex conjugate) prevent an exact solution for the dynamics an one instead applies a perturbative approach. Rather than perturb directly in this term, one typically includes the average $\langle Je^{G_1}e^{-G_2}\rangle$ in the zeroth-order Hamiltonian and perturbs in the difference $Je^{G_1}e^{-G_2} - \langle Je^{G_1}e^{-G_2}\rangle$. The average is with respect to an equilibrium phonon bath at the temperature of interest. (One is of course not *required* to include the average of the perturbation in the zeroth-order Hamiltonian but doing so only slightly adds to the computational effort and can greatly reduce the size of the perturbation.) The result is then $H = H_0 + V$, where

$$H_0 = \begin{pmatrix} H_B + \frac{\Delta}{2} - E_{p1} & \langle Je^{G_1}e^{-G_2}\rangle \\ \langle Je^{G_2}e^{-G_1}\rangle & H_B - \frac{\Delta}{2} - E_{p2} \end{pmatrix} \tag{4.13}$$

and

$$V = \begin{pmatrix} 0 & Je^{G_1}e^{-G_2} - \langle Je^{G_1}e^{-G_2}\rangle \\ Je^{G_2}e^{-G_1} - \langle Je^{G_2}e^{-G_1}\rangle & 0 \end{pmatrix}. \tag{4.14}$$

As the name suggests, the polaron transform was first used to study the motion of electrons in crystal lattices [21–24]. It has also been used to study energy transfer in the incoherent regime [25], and has recently been applied to the study of coherent resonance energy transfer [26–28].

The nature of this approximation is to first create polaron states composed of an exciton coupled to a cloud of phonons, and to then (approximately) consider energy transfer between these polaron states. As a result, the polaron transform is most effective when the coupling of each molecule to its environment is more important than the coupling between the molecules, just as in Förster theory. In fact, it is

worth pointing out that one can derive a special case of Förster theory directly from Eq. (4.11) by assuming uncoupled baths and applying Fermi's Golden Rule to treat the off-diagonal elements $Je^{G_1}e^{-G_2}$.

Finally, we note that if the spectral density of the bath is ohmic, the average $\langle Je^{G_1}e^{-G_2}\rangle$ is always exactly zero, regardless of how weak the system–bath coupling is. This means that the donor–acceptor coupling is entirely absent from the zeroth-order Hamiltonian and is only treated perturbatively; one therefore cannot capture donor–acceptor coherence at any reasonable order of perturbation. Aslangul et al. have studied the spin–boson model with ohmic spectral density using the polaron transform [29, 30].

4.3 Model

While many of the existing theories have been successful in limited parameter ranges, it is particularly desirable to develop a theory for energy transfer that can correctly describe the dynamics over a wide range of parameter values. Förster theory and related theories are perturbative in the electronic coupling and cannot correctly describe the coherent dynamics that result from strong coupling. On the other hand, many of the master equation approaches developed recently instead use the linear system–phonon coupling as a perturbation; these theories are of course unsuitable when the system–bath coupling becomes large, unless one can go to high order in the perturbation [14, 31–33].

In order to provide a second order perturbation method that will give good results in both the weak coupling and strong coupling limit, we will use the variational polaron method for such problems that was introduced by Yarkony and Silbey and used by Silbey and Harris [34–37]. Recently, we learned that McCutcheon and Nazir [38, 39] have also done a calculation with this method. Their results and ours coincide for the same parameter set.

We use the two-state Hamiltonian introduced earlier in Eq. (4.2) as our starting point. This Hamiltonian assumes linear coupling between the electronic states and

the bath, but is otherwise quite general. In particular, we have allowed both electronic states to interact with the same phonon modes; we can also treat the case of independent baths as a special case by requiring either g_{1k} or g_{2k} to be zero for each k such that each mode only couples to one of the electronic states, or have correlation between the modes on different sites.

Before proceeding to look in more detail at this system, we rewrite the Hamiltonian in the following form:

$$H = \begin{pmatrix} H_B + \frac{\Delta}{2} + B & J \\ J & H_B - \frac{\Delta}{2} - B \end{pmatrix}, \tag{4.15}$$

where

$$H_B = \sum_k \hbar\omega_k \left(b_k^\dagger b_k + \frac{1}{2} \right), \tag{4.16}$$

$$B = \sum_k \hbar\omega_k g_k (b_k^\dagger + b_k), \tag{4.17}$$

and

$$g_k = \frac{g_{1k} - g_{2k}}{2}. \tag{4.18}$$

We have simply written the Hamiltonian in a form where the coupling to the bath is treated in a symmetric manner. It is always possible to write a Hamiltonian of the form of Eq. (4.2) in this manner by performing a polaron transform

$$H \to e^{\bar{g}_k (b_k^\dagger - b_k)} H e^{-\bar{g}_k (b_k^\dagger - b_k)} \tag{4.19}$$

where

$$\bar{g}_k = \frac{1}{2}(g_{1k} + g_{2k}), \tag{4.20}$$

and by redefining the zero of energy if necessary. A nice feature of this Hamiltonian is that it does not depend on g_{1k} and g_{2k} individually, but only on their difference.

At this point, one could solve for the dynamics of this Hamiltonian by perturbing in the system–bath interaction, as was done by Redfield [17]. Alternatively, if the system–bath coupling is large, one could perform the polaron transform introduced

in Eq. (4.10) and instead perturb in $J\theta - J\langle\theta\rangle$. For ohmic spectral densities, $J\langle\theta\rangle$ is always zero and there is no coherence in the zeroth-order Hamiltonian; as a result, the polaron transform technique always yields completely incoherent dynamics and is qualitatively incorrect at small system–bath coupling. At large system–bath coupling, a polaron transform is required since directly perturbing in the large system–bath coupling will not yield good results.

In the case of intermediate system–bath coupling, it is not always clear which of these two approaches will yield better results. A method that can interpolate between the two limiting cases would thus be very useful, particularly at intermediate system–bath coupling. It is such a method that is presented here.

4.4 Variational polaron transform

4.4.1 Partial polaron transform

In the context of finding an appropriate perturbation for intermediate system–bath coupling, we now introduce the partial polaron transform. This partial polaron transform was first introduced by Yarkony and Silbey [34, 35], and later used by Harris and Silbey [36, 37]. Instead of choosing between a complete polaron transform and no polaron transform at all, one can only partially transform each of the phonon modes as follows,

$$e^{G\sigma_z} H e^{-G\sigma_z} \quad \text{where} \quad G = \sum_k f_k (b_k^\dagger - b_k), \tag{4.21}$$

for some set of parameters f_k. We note that choosing $f_k = g_k$ corresponds to performing a complete polaron transform as introduced earlier, while choosing $f_k = 0$ corresponds to performing no polaron transform at all. In general, the f_k will be between these two limits and we will only partially transform the phonon modes.

We then obtain

$$H = \begin{pmatrix} \frac{\Delta}{2} + B_d + H_B & Je^{2G} \\ Je^{-2G} & -\frac{\Delta}{2} - B_d + H_B \end{pmatrix} \tag{4.22}$$

where

$$B_d = \sum_k \hbar\omega_k g_{dk}(b_k^\dagger + b_k) \qquad \text{and} \qquad g_{dk} = g_k - f_k. \tag{4.23}$$

We note that there will be a polaron shift added to both states, but it will be of the same magnitude and sign for both states so we have not included it.

Our Hamiltonian is now in a suitable form for a perturbative expansion, $H = H_0 + V$. We take as our zeroth order Hamiltonian

$$H_0 = \begin{pmatrix} \frac{\Delta}{2} & J_p \\ J_p & -\frac{\Delta}{2} \end{pmatrix} \tag{4.24}$$

where $J_p = J\langle e^{2G}\rangle$ and the angle brackets indicate an average over the bath in thermal equilibrium.

Our perturbation is then:

$$V = \begin{pmatrix} B_d & Je^{2G} - J_p \\ Je^{-2G} - J_p & -B_d \end{pmatrix} \tag{4.25}$$

We note again that the thermal average of our perturbation is zero by explicit construction, just as it was in the full polaron case.

For later convenience, we will express the perturbation as

$$u_x V_x + u_y V_y + u_z V_z, \tag{4.26}$$

where the u_i act only on the bath subspace, and the $V_i = \sigma_i$ are Pauli matrices that act only in the system subspace. We will refer to the system operators as V_i rather than σ_i to avoid confusion with the reduced density matrix σ. Specifically, we have

$$u_x = \frac{J}{2}\left[e^{2G} + e^{-2G}\right] - J\langle e^{2G}\rangle, \tag{4.27}$$

$$u_y = \frac{iJ}{2}\left[e^{2G} - e^{-2G}\right], \tag{4.28}$$

and

$$u_z = B_d = \sum_k \hbar\omega_k g_{dj}(b_k^\dagger + b_k). \tag{4.29}$$

4.4.2 Variational condition

Our choice of H_0 and V depends on our choice of the parameters f_k; it will of course be desirable to choose the f_k in a manner that will minimize the perturbation V. It is clear from the variational principle of quantum mechanics that we will obtain the best ground state for our system by minimizing the ground state energy. We are, however, interested in dynamics among many states and it makes sense for our variational criterion to also include contributions from excited states of the system that will be populated at the temperature of interest. We will follow the suggestion of Silbey and Harris who suggested choosing the f_k such that the free energy of H_0 is a minimum [36].

Briefly, Gibbs and Bogoliubov have shown that upon partitioning a Hamiltonian as $H = H_0 + V$ and defining free energies

$$A = \beta^{-1}e^{-\beta H} \qquad A_0 = \beta^{-1}e^{-\beta H_0}, \tag{4.30}$$

one has

$$A \leq A_0 + \langle V \rangle_0, \tag{4.31}$$

where the average is with respect to the canonical distribution of H_0 [40]. As we have explicitly chosen V such that $\langle V \rangle_0 = 0$, we can ignore that term in the Gibbs–Bogoliubov inequality. Of course, at zero temperature our free energy bound becomes the well-known energy bound but at finite temperature it allows some contribution from excited states.

Choosing the f_k to minimize A_0 yields [37]

$$f_k = g_k \left\{ 1 + \frac{2J_p^2 \coth(\beta\omega_k/2) \tanh \beta\sqrt{\Delta^2 + J_p^2}}{\hbar\omega_k \sqrt{\Delta^2 + J_p^2}} \right\}^{-1}. \tag{4.32}$$

We note that J_p itself depends on our choice of f_k and so this equation is not an explicit formula for f_k, but rather a self-consistent equation. The main results of this chapter do not depend on the particular choice of f_k; while we will use Eq. (4.32) throughout the chapter, it may be interesting in the future to look at other criteria for minimizing the perturbation.

4.5 Perturbative solution of dynamics

4.5.1 Overview

The variational polaron transform introduced in the last section was used by Silbey and Harris to obtain some analytical results on the tunneling dynamics of optical isomers, which can be described by the same spin–boson Hamiltonian we are using here. The technique proved very powerful at predicting the transition from coherent to incoherent motion in these systems, and was used to obtain some very simple dynamics [36, 37]. Despite these early successes, an application of the variational polaron transform to the calculation of energy transfer dynamics has not been fully explored.

The development to this point has provided us with a zeroth-order Hamiltonian and a perturbation, which we can use to solve perturbatively for the dynamics. Several types of master equations have been used in the past to solve for the reduced density matrix of the system; we choose to apply the second-order time-convolutionless master equation, which we now write down in the form used by Ishizaki and Fleming [41],

$$\frac{d\tilde{\sigma}}{dt} = -\frac{1}{\hbar^2}\sum_{mn}\int_0^t ds V_m(t)^\times \left[S_{mn}(t-s)V_n(s)^\times - \frac{i\hbar}{2}\chi_{mn}(t-s)V_n(s)^\circ\right]\tilde{\sigma}(t). \quad (4.33)$$

All of the operators are in the interaction representation with respect to H_0 and we have introduced the notation $V^\times \equiv [V,\cdot]$ and $V^\circ \equiv \{V,\cdot\}$ for the commutator and anticommutator. The correlation functions $\chi(t)$ and $S(t)$ are defined as:

$$S_{mn}(t) \equiv \frac{1}{2}\langle\{u_m(t), u_n(0)\}\rangle \qquad \chi_{mn}(t) \equiv \frac{i}{\hbar}\langle[u_m(t), u_n(0)]\rangle, \quad (4.34)$$

where the averages are over a canonical distribution at the temperature of interest. Since all of the u_i are Hermitian, we have the property that

$$S_{nm}(t) = S_{mn}(-t) \qquad \text{and} \qquad \chi_{nm}(t) = -\chi_{mn}(-t), \tag{4.35}$$

and there are only 6 independent correlation functions.

A concise derivation of the time-convolutionless master equation is presented by Hashitsume [42], and it has frequently been used to study energy transfer [26, 41, 43]. Eq. (4.33) is an equation of motion for the reduced density matrix of the system in the interaction representation of H_0, $\tilde{\sigma}(t)$. We make a few observations about this equation

- The term $\tilde{\sigma}(t)$ is not affected by the integral over s—the equation is therefore time-local. (This is of course in contrast to the related *time-convolution* master equation.)
- The coefficient of $\tilde{\sigma}(t)$ in the master equation is time-dependent and the equation is thus non-Markovian.

In order to derive this form of the time-convolutionless master equation, one must assume that the bath is initially in equilibrium. Jang et al. have looked in detail at the effect of including the initial condition in the time-convolutionless master equation for a similar system; including the initial condition effects made some small changes to their results but did not qualitatively change the energy transfer dynamics [26]. It would nonetheless be interesting in the future to examine the effect of nonequilibrium initial state on the present theory.

4.5.2 Correlation functions

Many of the correlation functions needed to solve the time-convolutionless master equation are already known. In particular, the correlation functions of u_z are known from treating the problem without a polaron transform [41], while the correlation functions involving u_x and u_y are known from the theories which perform a full

polaron transform [26]. The cross-correlation functions between (u_x, u_y) and u_z are new to this work but can be computed straightforwardly.

In order to express these correlation functions, we define three new spectral densities in terms of the system–bath coupling terms and the variational parameters,

$$\eta_d(\omega) = \sum_j \omega_j^2 g_{dj}^2 \delta(\omega - \omega_j), \tag{4.36}$$

$$\eta_p(\omega) = \sum_j \omega_j^2 f_j^2 \delta(\omega - \omega_j), \tag{4.37}$$

and

$$\eta_m(\omega) = \sum_k \omega_k^2 f_k g_{dk} \delta(\omega - \omega_k). \tag{4.38}$$

All of the correlation functions can now be expressed in terms of these spectral densities. The correlation functions of u_x and u_y are expressed in terms of two auxiliary functions,

$$\mu(t) = 4 \int_0^\infty d\omega \frac{\eta_p(\omega) \sin(\omega t)}{\omega^2} \tag{4.39}$$

and

$$\nu(t) = 4 \int_0^\infty d\omega \frac{\eta_p(\omega) \cos(\omega t)}{\omega^2} \coth\left(\frac{\beta\hbar\omega}{2}\right). \tag{4.40}$$

As can be seen from the above equation, it is possible for the integral for $\nu(t)$ to diverge at small ω; in particular, this happens for ohmic spectral density. In the case where $\nu(0)$ and $\nu(t)$ are both infinite, but $\nu(0) - \nu(t)$ remains finite, we can still obtain finite correlation functions:

$$S_{xx}(t) = \frac{J^2}{2} \cos[\mu(t)] e^{-[\nu(0)-\nu(t)]} \tag{4.41}$$

$$\chi_{xx}(t) = \frac{J^2}{\hbar} \sin\left[\mu(t)\right] e^{-[\nu(0)-\nu(t)]} \tag{4.42}$$

$$S_{yy}(t) = \frac{J^2}{2} \cos\left[\mu(t)\right] e^{-[\nu(0)-\nu(t)]} \tag{4.43}$$

$$\chi_{yy}(t) = \frac{J^2}{\hbar} \sin\left[\mu(t)\right] e^{-[\nu(0)-\nu(t)]}. \tag{4.44}$$

In the case where $\nu(0)$ and $\nu(t)$ are both finite, we find that

$$S_{xx}(t) = J^2 e^{-\nu(0)} \left\{ \cos[\mu(t)] \cosh[\nu(t)] - 1 \right\} \tag{4.45}$$

$$\chi_{xx}(t) = \frac{2J^2 e^{-\nu(0)}}{\hbar} \sin[\mu(t)] \sinh[\nu(t)] \tag{4.46}$$

$$S_{yy}(t) = J^2 e^{-\nu(0)} \cos[\mu(t)] \sinh[\nu(t)] \tag{4.47}$$

$$\chi_{yy}(t) = \frac{2J^2 e^{-\nu(0)}}{\hbar} \sin[\mu(t)] \cosh[\nu(t)]. \tag{4.48}$$

Finally, $S_{xy}(t) = \chi_{xy}(t) = 0$ in all cases.

Turning now to the correlation functions of u_z, we obtain

$$S_{zz}(t) = \hbar^2 \int_0^\infty d\omega \eta_d(\omega) \cos(\omega t) \coth\left(\frac{\beta\hbar\omega}{2}\right) \tag{4.49}$$

and

$$\chi_{zz}(t) = 2\hbar \int_0^\infty d\omega \eta_d(\omega) \sin(\omega t). \tag{4.50}$$

Finally, we can obtain the cross-correlation functions between (u_x, u_y) and u_z as

$$S_{zy}(t) = 2\hbar J e^{-\nu(0)/2} \int d\omega \frac{\eta_m(\omega)}{\omega} \sin(\omega t) \coth(\beta\hbar\omega/2) \tag{4.51}$$

$$\chi_{zy}(t) = -4J e^{-\nu(0)/2} \int d\omega \frac{\eta_m(\omega)}{\omega} \cos(\omega t). \tag{4.52}$$

Both of the correlation functions $S_{zx}(t)$ and $\chi_{zx}(t)$ vanish. Finally, in the case where $\nu(0)$ is infinite, all of the cross-correlation functions vanish.

4.5.3 Commutators

The operators, $V_m(t)^\times$ and $V_n(t)^\circ$ are just commutators and anticommutators of Pauli matrices transformed to the interaction picture and are likewise easily computed. For completeness, we include these commutators in this section. All of the commutators are written in Liouville space in the basis $\{\sigma_x, \sigma_y, \sigma_z, I\}$ and all of the operators act in the basis of eigenstates of H_0. We have defined θ such that $J = \frac{\Delta}{2} \tan\theta$ and ω_e as

the exciton frequency, $\hbar^{-1}\sqrt{\Delta^2 + 4J_p^2}$.

The commutators of σ_x are:

$$\tilde{\sigma}_x(t)^{\times} = 2i \begin{pmatrix} 0 & -\sin\theta & -\cos\theta\sin\omega_e t & 0 \\ \sin\theta & 0 & -\cos\theta\cos\omega_e t & 0 \\ \cos\theta\sin\omega_e t & \cos\theta\cos\omega_e t & 0 & 0 \\ 0 & 0 & 0 & 0 \end{pmatrix} \tag{4.53}$$

and

$$\tilde{\sigma}_x(t)^{\circ} = 2 \begin{pmatrix} 0 & 0 & 0 & \cos\theta\cos\omega_e t \\ 0 & 0 & 0 & -\cos\theta\sin\omega_e t \\ 0 & 0 & 0 & \sin\theta \\ \cos\theta\cos\omega_e t & -\cos\theta\sin\omega_e t & \sin\theta & 0 \end{pmatrix} \tag{4.54}$$

The commutators of σ_y are:

$$\tilde{\sigma}_y(t)^{\times} = 2i \begin{pmatrix} 0 & 0 & \cos\omega_e t & 0 \\ 0 & 0 & -\sin\omega_e t & 0 \\ -\cos\omega_e t & \sin\omega_e t & 0 & 0 \\ 0 & 0 & 0 & 0 \end{pmatrix} \tag{4.55}$$

and

$$\tilde{\sigma}_y(t)^{\circ} = 2 \begin{pmatrix} 0 & 0 & 0 & \sin\omega_e t \\ 0 & 0 & 0 & \cos\omega_e t \\ 0 & 0 & 0 & 0 \\ \sin\omega_e t & \cos\omega_e t & 0 & 0 \end{pmatrix} \tag{4.56}$$

Finally, the commutators of σ_z are

$$\tilde{\sigma}_z(t)^{\times} = 2i \begin{pmatrix} 0 & -\cos\theta & \sin\theta\sin\omega_e t & 0 \\ \cos\theta & 0 & \sin\theta\cos\omega_e t & 0 \\ -\sin\theta\sin\omega_e t & -\sin\theta\cos\omega_e t & 0 & 0 \\ 0 & 0 & 0 & 0 \end{pmatrix} \tag{4.57}$$

and

$$\tilde{\sigma}_z(t)^\circ = 2 \begin{pmatrix} 0 & 0 & 0 & -\sin\theta\cos\omega_e t \\ 0 & 0 & 0 & \sin\theta\sin\omega_e t \\ 0 & 0 & 0 & \cos\theta \\ -\sin\theta\cos\omega_e t & \sin\theta\sin\omega_e t & \cos\theta & 0 \end{pmatrix} \tag{4.58}$$

We now have all of the required pieces in order to compute energy transfer dynamics using Eq. (4.33).

4.6 Results

4.6.1 Ohmic bath

We will now apply the theory outlined here to a few cases of interest. Recently, Ishizaki and Fleming have looked at the rate of energy transfer as a function of system–bath coupling using several of the existing theories [41]. We will use the same parameters as they did so that our results can be compared to theirs. In particular, we will choose $\Delta = 100$ cm^{-1}, $J = 20$ cm^{-1}, and $T = 300$ K. The two sites are coupled to independent bath modes with the same spectral density

$$\eta_{1(2)}(\omega) \equiv \sum_k \omega_k^2 g_{k1(2)}^2 \delta(\omega - \omega_k) = \frac{2\hbar\lambda\omega}{\pi\gamma} \frac{\gamma^2}{\omega^2 + \gamma^2}, \tag{4.59}$$

for $\gamma = 53$ cm^{-1}. We will examine the dynamics for various values of λ, which is the reorganization energy of the bath.

For these parameters, the dynamics are mainly incoherent and thus it makes sense to define a rate of population transfer. In Fig. 4-1, we plot the rate of population transfer from site 1 to site 2 as a function of reorganization energy, calculated using the variational polaron transform method outlined here. For comparison, we also plot the results obtained by performing a full polaron transform and by performing no polaron transform. (The case of no polaron transform was considered by Ishizaki and Fleming and our results agree with theirs [41].) As expected, the results obtained without

performing a polaron transform are qualitatively incorrect at large reorganization energy, but the polaron transform result correctly shows a decreasing rate as the reorganization energy becomes very large.

More interestingly, the variational polaron transform interpolates between these results and obtains reasonable results for all values of the reorganization energy. Our variational polaron transfer rates are very similar to those obtained using the hierarchical equation approach of Ishizaki and Fleming [41]. We also point out that for these parameters, the full polaron transform actually predicts the transfer rates quite well over the whole range of reorganization energies considered, but the variational technique does introduce some minor corrections at small λ.

Finally, we note that for $\lambda \gtrsim 5$ cm^{-1} the variational polaron results are identical to the full polaron results. This is because for large enough reorganization energy the solution to the variational condition, Eq. (4.32), is $J_p = 0$ and $f_k = g_k$; thus a full polaron transform is performed even in the variational calculation. As was shown analytically by Silbey and Harris, J_p does not go continuously to zero but does so abruptly when a critical value of λ is reached. It is for this reason that we see a discontinuous jump around $\lambda = 5$ cm^{-1} in the rates predicted by the variational calculation.

Next, we consider a case where coherence is important by setting $J = 100$ cm^{-1} and leaving all other parameters the same (again following Ishizaki and Fleming [41]). Since the energy transfer has coherent oscillations in this case, it is not as useful to think about a rate of energy transfer and we instead look the dynamics as a function of time when the system is started in state 1. Fig. 4-2 shows the population of site 1 as a function of time for four different values of the reorganization energy, λ.

For the two smallest values of the reorganization energy, the results obtained from the variational polaron transform are essentially identical to those obtained without performing a polaron transform. These results are in reasonable agreement with those obtained by Ishizaki and Fleming using the hierarchical techniques developed by Tanimura and Kubo [32, 33, 41]. We point out that for these two cases, the full polaron result is qualitatively incorrect, yielding unphysical results for $\lambda = 2$ cm^{-1}

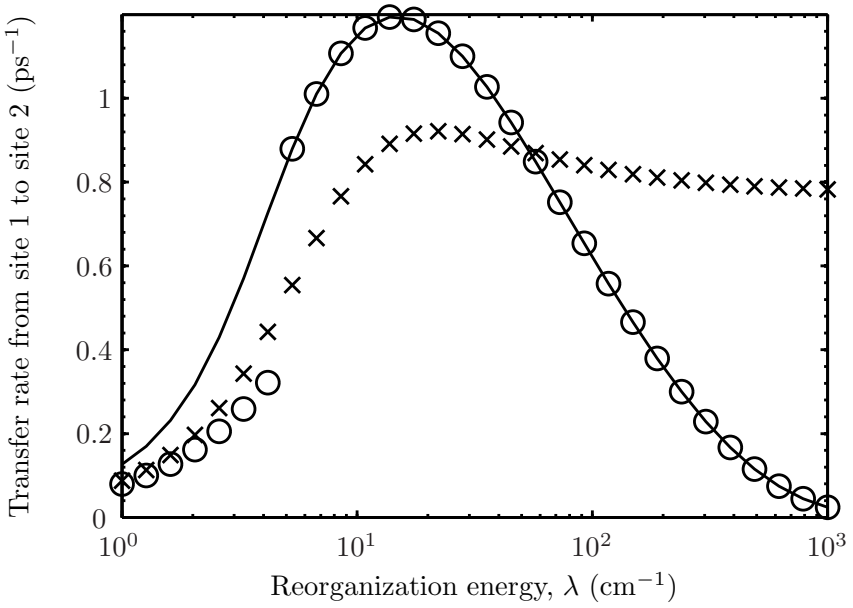

Figure 4-1: Rate of population transfer as a function of reorganization energy for a dimer with asymmetry $\Delta = 100$ cm^{-1}, coupling $J = 20$ cm^{-1}, ohmic spectral density as in Eq. (4.59) with inverse bath correlation time $\gamma = 53$ cm^{-1}, and temperature $T = 300$ K. The solid line is calculated by performing a full polaron transform, the crosses are calculated without performing a polaron transform, and the open circles are calculated using the variational technique explained in the text.

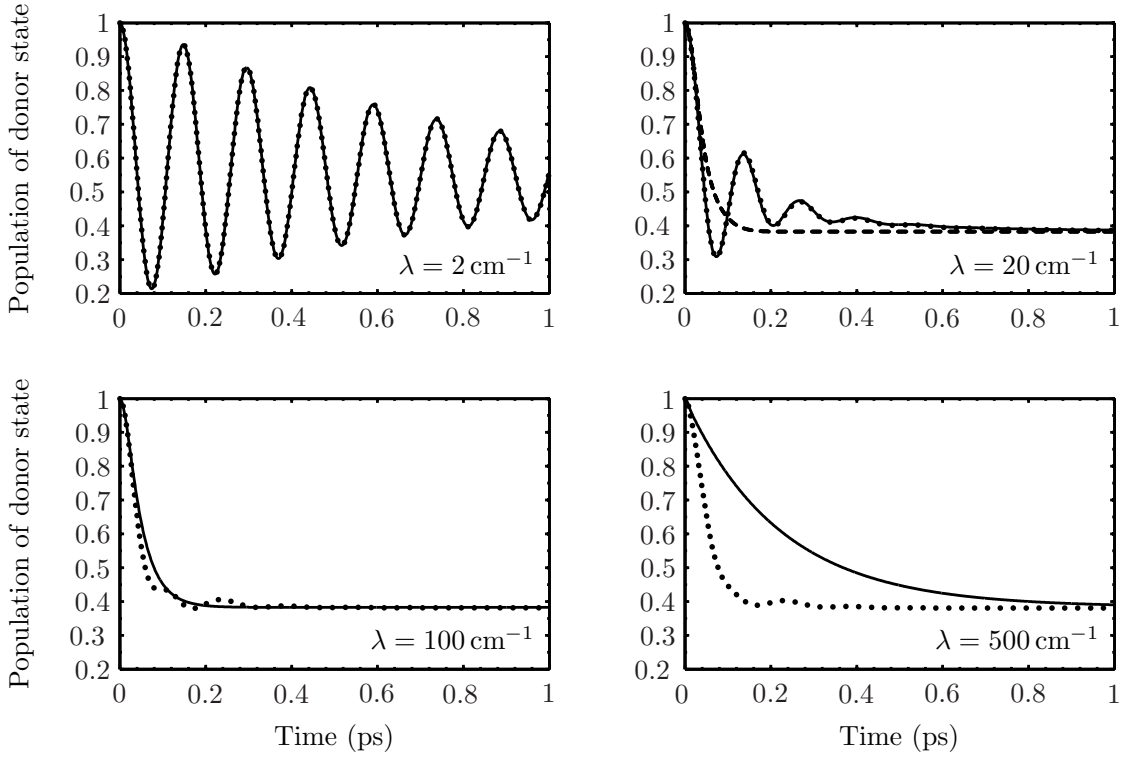

Figure 4-2: Population of donor state as a function of time for a dimer with asymmetry $\Delta = 100$ cm^{-1}, coupling $J = 100$ cm^{-1}, ohmic spectral density as in Eq. (4.59) with inverse bath correlation time $\gamma = 53$ cm^{-1}, and temperature $T = 300$ K. The dynamics are plotted for four different values of the bath reorganization energy λ. The dotted line is computed without performing a polaron transform, while the solid line is computed using the variational polaron transform introduced in the text. The dashed line for $\lambda = 20$ cm^{-1} is computed using a full polaron transform. (The full polaron transform result is not included on the other plots as it yields unphysical results for $\lambda = 2$ cm^{-1} and is identical to the variational result for $\lambda = 100$ cm^{-1} and $\lambda = 500$ cm^{-1}.)

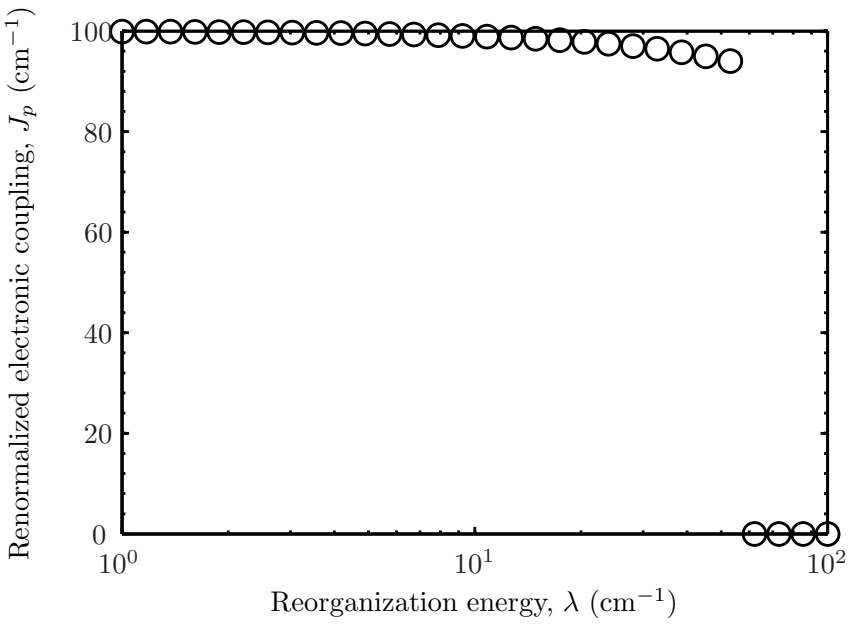

Figure 4-3: Renormalized electronic coupling, J_p as a function of reorganization energy for a dimer with asymmetry $\Delta = 100$ cm^{-1}, coupling $J = 100$ cm^{-1}, ohmic spectral density as in Eq. (4.59) with inverse bath correlation time $\gamma = 53$ cm^{-1}, and temperature $T = 300$ K. J_p is computed using the variational polaron transformation described in the text.

and failing to predict any coherence for $\lambda = 20$ cm^{-1}.

For the two largest values of reorganization energy, the variational result is the same as the full polaron transform result, for the reasons discussed earlier. These polaron transform dynamics correctly show a decrease in the rate of energy transfer at large reorganization energy. In contrast, the results without a polaron transform show a qualitatively incorrect timescale for large reorganization energy, as was also seen in Fig. 4-1. We also note that the results from Ishizaki and Fleming's hierarchical technique show non-exponential kinetics at short times as well as a few coherent oscillations at $\lambda = 100$ cm^{-1} that are not reproduced by our variational technique. Nonetheless, the overall timescale of population transfer from our method agrees quite well with that of Ishizaki and Fleming [41].

Finally, we note that for the parameters in Fig. 4-2, the variational method always yields results that are identical to either performing a full polaron transform or not performing a polaron transform. We emphasize, however, that this is not always

the case; in particular, our results at low reorganization in Fig. 4-1 show that the variational method can indeed give results distinct from the two limiting cases.

In general, we expect the variational method to be distinct from the two limiting cases when J_p is intermediate between 0 and J. When the reorganization energy is zero, $J_p = J$; as the reorganization energy increases, J_p decreases continuously until a critical reorganization energy is reached, at which point J_p jumps discontinuously to zero. As a concrete example, Fig. 4-3 plots J_p vs. reorganization energy for the same parameters as in Fig. 4-2.

For these particular parameters, we see that J_p has barely decreased from J before this discontinuous jump and thus J_p is never truly intermediate between 0 and J; the variational method thus always essentially reproduces one of the limiting cases. For other parameters (such as those in Fig. 4-1), J_p does decrease significantly from J before jumping to zero; for those parameters where J_p is intermediate, the variational calculation will yield results that are distinct from both limiting cases.

4.6.2 Superohmic bath

We now demonstrate the general applicability of our method by using it to treat a system with a superohmic bath. Again, in order to compare our new method with existing methods in the literature, we choose the same parameters as Jang et al. [26]. In particular, we consider a dimer coupled to a bath with spectral density

$$\eta_d(\omega) = \frac{\eta\omega^3}{6\omega_c^2} e^{-\omega/\omega_c}, \tag{4.60}$$

in units where $\hbar = \omega_c = k_B T = 1$. In this case, we are allowing correlated fluctuations between the two sites, so there is a single bath with the above spectral density to which both electronic states couple. Starting with an initially excited donor state, we plot the population of the donor state as a function of time for various values of the energy difference Δ and electronic coupling J. The results are presented for two values of η—in Fig. 4-4, we present the results for $\eta = 1$ while in Fig. 4-5 we present the results for $\eta = 3$. Our results for the full polaron calculation are of course

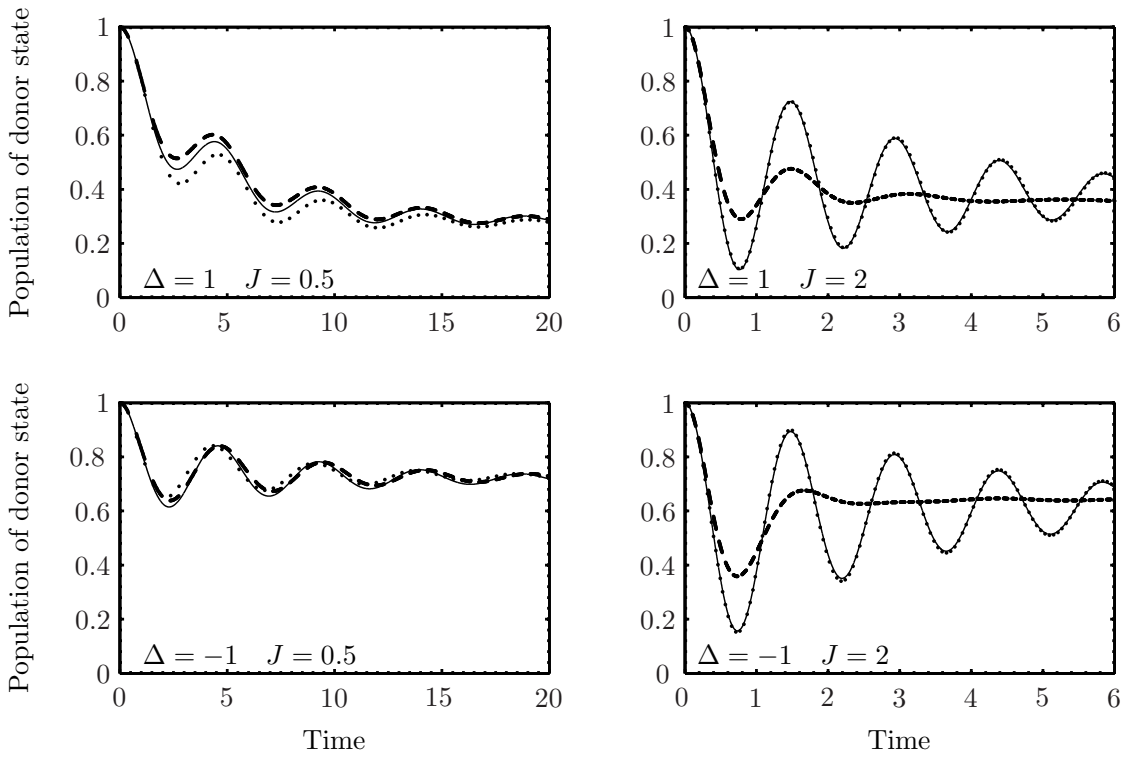

Figure 4-4: Population of donor state as a function of time for a dimer coupled to a bath with superohmic spectral density given by Eq. (4.60) with $\eta = 1$. The dynamics are plotted for four different values of the energy splitting Δ and coupling J, as indicated on each figure. The dotted line is computed without performing a polaron transform, the dashed line for is computed using a full polaron transform, and the solid line is computed using the variational polaron transform introduced in the text. Units are such that $\hbar = \omega_c = k_B T = 1$.

identical to those of Jang et al. but we also present results for the case of no polaron transform and for the variational polaron transform.

We now make several observations about these results. For the two graphs on the left side of Fig. 4-4, where $\Delta = \pm 1$ and $J = 0.5$, we see that all three results are very similar. For these parameters, both the electronic copuling J and the system–bath coupling are less significant than the energy splitting Δ and it does not make a large difference which perturbation one chooses. In contrast to the results for ohmic spectral density, the full polaron transform preserves donor–acceptor coherence for weak enough system–bath coupling. Turning now to the two graphs on the right side of Fig. 4-4, we see that for this larger value of J the full-polaron and no-polaron trans-

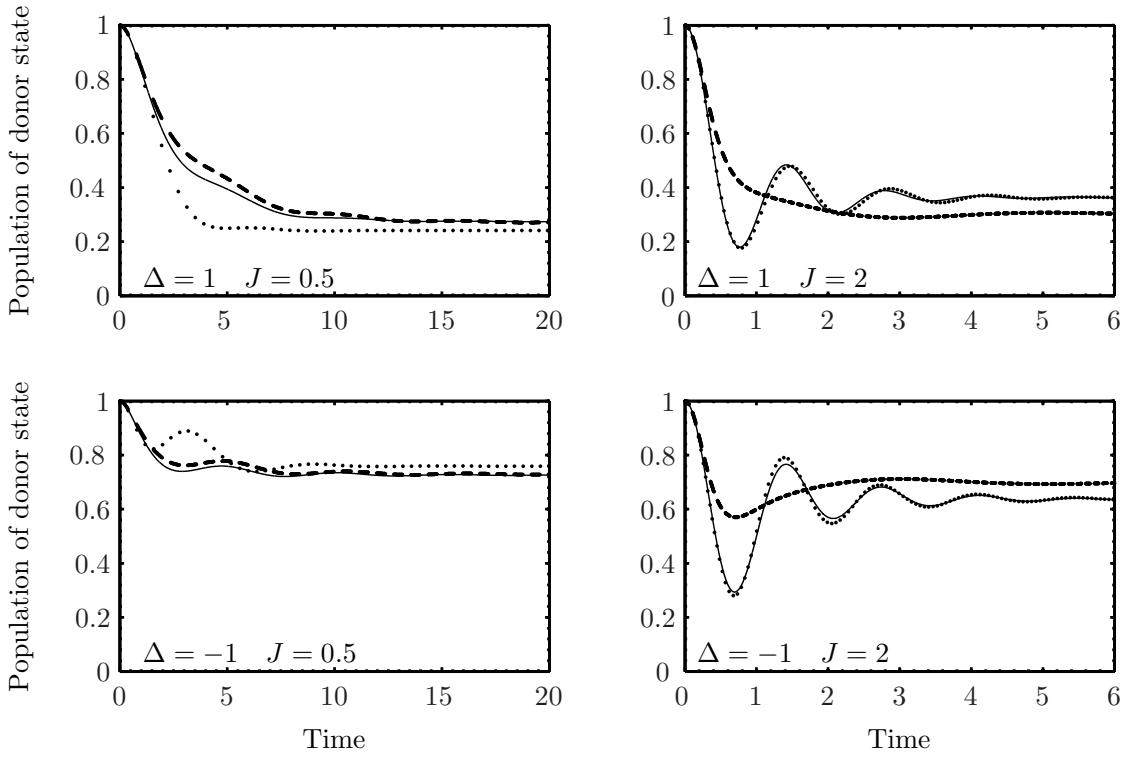

Figure 4-5: Population of donor state as a function of time for a dimer coupled to a bath with superohmic spectral density given by Eq. (4.60) with $\eta = 3$. The dynamics are plotted for four different values of the energy splitting Δ and coupling J, as indicated on each figure. The dotted line is computed without performing a polaron transform, the dashed line for is computed using a full polaron transform, and the solid line is computed using the variational polaron transform introduced in the text. Units are such that $\hbar = \omega_c = k_B T = 1$.

form results are significantly different. The variational result is essentially identical to the results obtained without performing a polaron transform, suggesting that this is the better perturbation for these particlar parameters.

For the larger system–bath coupling $\eta = 3$, there is a difference between the full-polaron and no-polaron transform results at $\Delta = \pm 1$ and $J = 0.5$, as seen in the graphs on the left side of Fig. 4-5. For these parameters, the variational polaron transform yields results similar to, but not identical to, those obtained from the full polaron transform. Just as in Fig. 4-4, upon moving to larger donor–acceptor coupling J we observe that the variational results approach those obtained without performing a polaron transform.

Our results for $J = 2$ suggest that coherence plays a larger role for these particular parameters than the polaron-transformed result would suggest. As discussed earlier, the polaron-transformed result should perform better when the system–bath coupling is more important than the electronic coupling; conversely, the results without a polaron transform should perform better when the electronic coupling is dominant. For the intermediate parameters considered here, it would be difficult to predict which of the two perturbations should yield better results, but the variational polaron transform provides an objective method of selecting a suitable perturbation. The results are particularly interesting in that they suggest that many of the situations treated with a polaron transform by Jang et al. might actually be better studied without a polaron transform.

We also observe in Figs. 4-4 and 4-5 that the eventual equilibrium state of the system depends somewhat on the particular perturbation chosen. This dependence is of course expected as the zeroth-order Hamiltonian largely controls the eventual equilibrium state. This result suggests that if one knows the expected equilibrium state, it may be possible to use such knowledge to help select the best perturbation.

4.7 Conclusion

We have presented a method for computing the dynamics of excitonic energy transfer that combines a variational polaron transform with the second-order time-convolutionless master equation. By variationally minimizing the perturbation, we were able to apply a second-order master equation to obtain energy transfer dynamics at small, intermediate, and large reorganization energies from a single theory. Our theory has the advantage of being conceptually simple and easily computable while still being applicable over a wide range of parameter values. The theory does leave room for improvement, as the variational minimization often rapidly jumps between no polaron transform and a full polaron transform, with intermediate transformations only occurring in limited parameter ranges. It would be interesting to examine alternate variational criteria with the goal of improving performance in the intermediate system–bath coupling regime.

Bibliography

[1] R. Kubo. Note on the stochastic theory of resonance absorption. *J. Phys. Soc. Japan* **9**, 935 (1954).

[2] R. Kubo and K. Tomita. A general theory of magnetic resonance absorption. *J. Phys. Soc. Japan* **9**, 888 (1954).

[3] H. Haken and P. Reineker. The coupled coherent and incoherent motion of excitons and its influence on the line shape of optical absorption. *Z. Phys. A: Hadrons Nucl.* **249**, 253 (1972).

[4] H. Haken and G. Strobl. An exactly solvable model for coherent and incoherent exciton motion. *Z. Phys. A: Hadrons Nucl.* **262**, 135 (1973).

[5] X. Chen and R. J. Silbey. Effect of correlation of local fluctuations on exciton coherence. *J. Chem. Phys.* **132**, 204503 (2010).

[6] R. W. Munn and R. Silbey. Theory of exciton transport with quadratic exciton–phonon coupling. *J. Chem. Phys.* **68**, 2439 (1978).

[7] T. Renger and R. A. Marcus. On the relation of protein dynamics and exciton relaxation in pigment–protein complexes: An estimation of the spectral density and a theory for the calculation of optical spectra. *J. Chem. Phys.* **116**, 9997 (2002).

[8] F. Müh, M. E.-A. Madjet, and T. Renger. Structure-based identification of energy sinks in plant light-harvesting complex II. *J. Phys. Chem. B* **114**, 13517 (2010).

[9] T. Brixner, J. Stenger, H. M. Vaswani, M. Cho, R. E. Blankenship, and G. R. Fleming. Two-dimensional spectroscopy of electronic couplings in photosynthesis. *Nature* **434**, 625 (2005).

[10] A. J. Leggett, S. Chakravarty, A. T. Dorsey, M. P. A. Fisher, A. Garg, and W. Zwerger. Dynamics of the dissipative two-state system. *Rev. Mod. Phys.* **59**, 1 (1987).

[11] R. L. Fulton and M. Gouterman. Vibronic coupling. I. Mathematical treatment for two electronic states. *J. Chem. Phys.* **35**, 1059 (1961).

[12] H. Hossein-Nejad and D. Scholes, Gregory. Energy transfer, entanglement and decoherence in a molecular dimer interacting with a phonon bath. *New J. Phys.* **12**, 065045 (2010).

[13] G. Bartłomiej. Exact solution of the Schrödinger equation with the spin–boson Hamiltonian. *J. Phys. A: Math. Theor.* **44**, 195301 (2011).

[14] A. Ishizaki and G. R. Fleming. Unified treatment of quantum coherent and incoherent hopping dynamics in electronic energy transfer: Reduced hierarchy equation approach. *J. Chem. Phys.* **130**, 234111 (2009).

[15] J. Strumpfer and K. Schulten. The effect of correlated bath fluctuations on exciton transfer. *J. Chem. Phys.* **134**, 095102 (2011).

[16] A. Nazir. Correlation-dependent coherent to incoherent transitions in resonant energy transfer dynamics. *Phys. Rev. Lett.* **103**, 146404 (2009).

[17] A. G. Redfield. On the theory of relaxation processes. *IBM J. Res. Dev.* **1**, 19 (1957).

[18] M. Yang and G. R. Fleming. Influence of phonons on exciton transfer dynamics: comparison of the Redfield, Förster, and modified Redfield equations. *Chem. Phys.* **282**, 163 (2002).

[19] V. I. Novoderezhkin, M. A. Palacios, H. van Amerongen, and R. van Grondelle. Energy-transfer dynamics in the LHCII complex of higher plants: Modified Redfield approach. *J. Phys. Chem. B* **108**, 10363 (2004).

[20] A. Ishizaki and G. R. Fleming. On the adequacy of the Redfield equation and related approaches to the study of quantum dynamics in electronic energy transfer. *J. Chem. Phys.* **130**, 234110 (2009).

[21] T. Holstein. Studies of polaron motion: Part I. The molecular-crystal model. *Ann. Phys.* **8**, 325 (1959).

[22] T. Holstein. Studies of polaron motion: Part II. The "small" polaron. *Ann. Phys.* **8**, 343 (1959).

[23] M. Grover and R. Silbey. Exciton migration in molecular crystals. *J. Chem. Phys.* **54**, 4843 (1971).

[24] M. K. Grover and R. Silbey. Exciton–phonon interactions in molecular crystals. *J. Chem. Phys.* **52**, 2099 (1970).

[25] S. Rackovsky and R. Silbey. Electronic energy transfer in impure solids I. Two molecules embedded in a lattice. *Mol. Phys.* **25**, 61 (1973).

[26] S. Jang, Y.-C. Cheng, D. R. Reichman, and J. D. Eaves. Theory of coherent resonance energy transfer. *J. Chem. Phys.* **129**, 101104 (2008).

[27] S. Jang. Theory of coherent resonance energy transfer for coherent initial condition. *J. Chem. Phys.* **131**, 164101 (2009).

[28] S. Jang. Theory of multichromophoric coherent resonance energy transfer: A polaronic quantum master equation approach. *J. Chem. Phys.* **135**, 034105 (2011).

[29] C. Aslangul, N. Pottier, and D. Saint-James. Quantum ohmic dissipation: Coherence vs. incoherence and symmetry-breaking. A simple dynamical approach. *J. Phys. (Paris)* **46**, 2031 (1985).

[30] C. Aslangul, N. Pottier, and D. Saint-James. Quantum ohmic dissipation: Transition from coherent to incoherent dynamics. *Phys. Lett. A* **110**, 249 (1985).

[31] J. Cao. A phase-space study of Bloch–Redfield theory. *J. Chem. Phys.* **107**, 3204 (1997).

[32] Y. Tanimura and R. Kubo. Time evolution of a quantum system in contact with a nearly Gaussian–Markoffian noise bath. *J. Phys. Soc. Japan* **58**, 101 (1989).

[33] Y. Tanimura. Stochastic Liouville, Langevin, Fokker–Planck, and master equation approaches to quantum dissipative systems. *J. Phys. Soc. Japan* **75**, 082001 (2006).

[34] D. Yarkony and R. Silbey. Comments on exciton phonon coupling: Temperature dependence. *J. Chem. Phys.* **65**, 1042 (1976).

[35] D. R. Yarkony and R. Silbey. Variational approach to exciton transport in molecular crystals. *J. Chem. Phys.* **67**, 5818 (1977).

[36] R. Silbey and R. A. Harris. Variational calculation of the dynamics of a two level system interacting with a bath. *J. Chem. Phys.* **80**, 2615 (1984).

[37] R. A. Harris and R. Silbey. Variational calculation of the tunneling system interacting with a heat bath. II. Dynamics of an asymmetric tunneling system. *J. Chem. Phys.* **83**, 1069 (1985).

[38] D. P. McCutcheon and A. Nazir. Consistent treatment of coherent and incoherent energy transfer dynamics using a variational master equation. *J. Chem. Phys.* **135**, 114501 (2011).

[39] D. P. S. McCutcheon, N. S. Dattani, E. M. Gauger, B. W. Lovett, and A. Nazir. A general approach to quantum dynamics using a variational master equation: Application to phonon-damped Rabi rotations in quantum dots. *Phys. Rev. B* **84**, 081305 (2011).

[40] M. D. Girardeau and R. M. Mazo. Variational methods in statistical mechanics. In *Advances in Chemical Physics*, I. Prigogine and S. A. Rice, Eds. , volume 24 (Wiley, New York, 1973), pp. 187–255.

[41] A. Ishizaki, T. R. Calhoun, G. S. Schlau-Cohen, and G. R. Fleming. Quantum coherence and its interplay with protein environments in photosynthetic electronic energy transfer. *Phys. Chem. Chem. Phys.* **12**, 7319 (2010).

[42] N. Hashitsume, F. Shibata, and M. Shingū. Quantal master equation valid for any time scale. *J. Stat. Phys.* **17**, 155 (1977).

[43] D. P. S. McCutcheon and A. Nazir. Coherent and incoherent dynamics in excitonic energy transfer: Correlated fluctuations and off-resonance effects. *Phys. Rev. B* **83**, 165101 (2011).

Chapter 5

Alternative Variational Transformations

5.1 Introduction

Chapter 4 presented a technique for studying coherent energy transfer by applying a variational polaron transform to a spin–boson Hamiltonian. As a result, this method was able to produce reasonable results for energy transfer dynamics over a wide range of parameters. In particular, the model appropriately selected to perturb in the bath for small system–bath coupling and to perform a polaron transform for large system–bath coupling. For intermediate system–bath coupling, a partial polaron transform was performed, although this partial polaron transform sometimes differed only slightly from either a full polaron transform or no polaron transform.

While these results are certainly very promising, they also leave some room for improvement. In particular, the transition from no polaron transform to a full polaron transform was quite abrupt, particularly for ohmic spectral densities. As a result, while the model gives reasonable results for all parameters examined, there is not a large region of parameter space where the model produces results that could not have been obtained from existing theories. Also, comparison to the exact results available for ohmic spectral densities [1] showed that while our theory certainly produces good results over a wide range of parameters, there are some noticeable differences between

our results and the exact results. In particular, our theory produced completely incoherent dynamics for parameters where the exact calculation shows some oscillations in the energy transfer.

One aspect of the variational polaron transform that was pointed out in Chapter 4 is that the particular transformation chosen affects the equilibrium state to which the system eventually relaxes. Recently, Moix and coworkers have developed a path-integral method for efficiently computing the exact equilibrium reduced density matrix of a system in contact with a harmonic bath [2]. This method has since been applied to study the equilibrium density matrix for the same spin–boson model we used in Chapter 4. In particular, Lee and coworkers compared the equilibrium density matrix predicted by the variational polaron transform to that obtained from the exact calculation [3]. While they examined only superohmic spectral densities, their results agree largely with the observations in the last chapter—the variational polaron transform approximately predicts the correct equilibrium state for all parameters considered, but does comparatively poorly in the intermediate system–bath coupling regime. Given these recent results, it is thus reasonable to suppose that using a known equilibrium state as input to the calculation could improve the results.

5.2 Polaron transformation

Our starting Hamiltonian will be the same as that in the last chapter,

$$H = \begin{pmatrix} H_B + \frac{\Delta}{2} + B & J \\ J & H_B - \frac{\Delta}{2} - B \end{pmatrix}, \tag{5.1}$$

with bath Hamiltonian

$$H_B = \sum_k \hbar\omega_k \left(b_k^\dagger b_k + \frac{1}{2} \right) \tag{5.2}$$

and system–bath coupling

$$B = \sum_k \hbar\omega_k g_k (b_k^\dagger + b_k). \tag{5.3}$$

Upon performing a partial polaron transform, we arrive at the form $H = H_0 + V$, with

$$H_0 = \begin{pmatrix} \frac{\Delta}{2} & J_p \\ J_p & -\frac{\Delta}{2} \end{pmatrix} \tag{5.4}$$

and

$$V = \begin{pmatrix} B_d & Je^{2G} - J_p \\ Je^{-2G} - J_p & -B_d \end{pmatrix}. \tag{5.5}$$

We have defined

$$B_d = \sum_k \hbar\omega_k g_{dk}(b_k^\dagger + b_k), \tag{5.6}$$

$$G = \sum_k f_k(b_k^\dagger - b_k), \tag{5.7}$$

$$g_{dk} = g_k - f_k, \tag{5.8}$$

and $J_p = J\langle e^{2G}\rangle$. The angle brackets indicate an average over the bath in thermal equilibrium.

At this point, the f_j in the polaron transform are arbitrary. While the last chapter always used the Gibbs–Bogoliubov free energy bound to select the optimal values of f_j, the method is not restricted to that particular choice of variational condition. In fact, one is free to choose the f_j in any desired manner; one can think of performing a full polaron transform as prescribing $f_j = g_j$ for all j, and performing no polaron transform as prescribing $f_j = 0$ for all j. Here, we will use the exact equilibrium reduced density matrix in order to inform our choice of f_j.

Given the equilibrium reduced density matrix of a system, ρ_{eq}, we can define an effective Hamiltonian as

$$H_{\text{eff}} = -\beta^{-1} \log \rho_{\text{eq}} = \frac{\Delta_{\text{eff}}}{2}\sigma_z + J_{\text{eff}}\sigma_x, \tag{5.9}$$

where β^{-1} is the temperature of the system. Romero-Rochin and Oppenheim have used projection operators to study in detail the dynamics of a system in contact with a bath; they have shown that it is not always possible to write the equilibrium reduced density matrix of the system in terms of an effective system Hamiltonian

[4]. In cases where the system and bath are taken to be initially uncorrelated, as is assumed here, this concern does not arise. Furthermore, we will not be using the results of Eq. (5.9) as an effective Hamiltonian, but rather to guide our choice of zeroth-order Hamiltonian and perturbation.

Our goal will be to select the f_j in our partial polaron transform such that the zeroth-order Hamiltonian H_0 is as close as possible to H_{eff}. Our variational transformation as written cannot change the energy splitting between the two states—we see from Eq. (5.4) that the zeroth-order Hamiltonian always has the same energy splitting Δ as the original system. One could use a more general polaron transform, such as by allowing the displacements on the two sites to have different magnitudes as has been considered by Allen and Silbey [5]. (This in contrast to the transformation considered here, where the displacements on the two sites are $\pm f_j$ and thus have the same magnitude but opposite signs.) Such a more general transformation would allow the energy splitting in the zeroth-order Hamiltonian to deviate from Δ.

In many cases of interest, however, the effective Hamiltonian has approximately the same splitting as the original Hamiltonian, even for large system–bath coupling. This is largely due to the symmetric form that we have chosen for the Hamiltonian—each bath mode couples to the two sites with equal magnitude but opposite sign. (Remembering of course that we showed in Chapter 4 that a more general system can always be transformed into this form.) As such, we will for the moment ignore any small changes in the effective splitting Δ_{eff} and focus on selecting the f_j such that electronic coupling in the zeroth-order Hamiltonian matches that in H_{eff}. In other words, we will attempt to select f_j such that $J_p = J_{\text{eff}}$.

Of course, our system is highly overdetermined—we can vary infinitely many parameters f_j in order to make J_p achieve its desired value. As such, we will impose further restrictions on the f_j. We found in the last chapter that the Gibbs-Bogoliubov bound produced the optimal f_j as

$$f_j = g_j \left\{ 1 + \frac{2J_p^2 \coth\left(\beta\omega_j/2\right) \tanh \beta\sqrt{\Delta^2 + J_p^2}}{\hbar\omega_j \sqrt{\Delta^2 + J_p^2}} \right\}^{-1}. \tag{5.10}$$

The first thing we notice about this result is that the system–bath coupling for each mode, g_j, enters only as a multiplicative factor. The relative displacement of each mode, $\zeta_j \equiv f_j/g_j$, is then a function of only ω_j and of a few overall system parameters. (Of course, J_p itself depends on the properties of each mode, but once it has been determined we can view it as a single parameter of the system.)

Here, we focus on the dependence of ζ_j on ω_j. As ω_j increases from 0 to infinity, ζ_j increases from 0 to 1. This behavior is not surprising, as it means that we generally directly perturb in low frequency modes and treat higher-frequency modes via polaron transform. Looking at the small and large ω_j limits, we obtain

$$\zeta(\omega) \sim \omega^2 \qquad \omega \to 0 \tag{5.11}$$

and

$$\zeta(\omega) \to 1 \qquad \omega \to \infty. \tag{5.12}$$

We are of course not required to choose a form of $\zeta(\omega)$ that matches that produced by the Gibbs-Bogoliubov bound; nonetheless, we choose to do so since such behavior is physically reasonable and produced good results in the last chapter. A simple functional form that exhibits the general behavior just enumerated is

$$\zeta(\omega) = \tanh^2(\alpha\omega). \tag{5.13}$$

Here α is a parameter that will be varied in an attempt to satisfy $J_p = J_{\text{eff}}$.

We can explicitly compute the average $J\langle e^{2G}\rangle$ in order to write J_p in terms of $\zeta(\omega)$ and the spectral density $\eta(\omega)$ as

$$J_p = J \exp\left[-2\int_0^\infty \frac{d\omega}{\omega^2}\eta(\omega)\tanh^2(\alpha\omega)\coth\left(\frac{\beta\hbar\omega}{2}\right)\right]. \tag{5.14}$$

For $\alpha = 0$, we obtain $J_p = J$; we have of course not performed a polaron transform in this case. For finite $\alpha > 0$, the integrand is positive and we always obtain $J_p < J$.

For ohmic spectral density, the integral would diverge at $\omega \to 0$ if not for the term

$\tanh^2(\alpha\omega)$, which exactly cancels the divergence for any value of $\alpha < \infty$. This means, however, that the integral will diverge in the limit $\alpha \to 0$, and that and $J_p \to 0$ in this limit. (This is of course the limit of performing a full polaron transform, where it is well known that the renormalized coupling $J_p = 0$.) For ohmic spectral density, then, we know that for any J_{eff} satisfying $0 < J_{\text{eff}} < J$ there will be an α such that $J_p = J_{\text{eff}}$.

For superohmic spectral density, the integral remains finite as $\alpha \to \infty$ (provided of course that we suitably cut off the spectral density $\eta(\omega)$ at large ω). This means that there is some minimum value of J_p; if J_{eff} is less than this minimum, there will be no value of α that can satisfy $J_p = J_{\text{eff}}$. Nonetheless, for all of the cases we considered, a suitable value of α can be found.

It is a simple matter to numerically determine the value of α required such that $J_p = J_{\text{eff}}$. The partial polaron transform is then fully defined and one can then use the partitioning of the Hamiltonian in Eq. (5.4) and (5.5) in any perturbative quantum dynamics.

5.3 Results

Here, we present some results for the dynamics and rate of energy transfer obtained using the partial polaron transformation described in the last section. Just as in Chapter 4, the dynamics are computed using the time-convolutionless master equation.

First, we look at the rate of energy transfer for a dimer with splitting $\Delta = 100$ cm^{-1} and coupling $J = 20$ cm^{-1}. Each site is independently coupled to a bath with Drude–Lorentz spectral density,

$$\eta(\omega) = \frac{2\hbar\lambda\omega}{\pi\gamma}\frac{\gamma^2}{\omega^2 + \gamma^2}, \tag{5.15}$$

with $\gamma = 100$ cm^{-1}, and the temperature is $T = 300$ K. The dynamics are largely incoherent for these parameters, and Fig. 5-1 shows the rate of energy transfer as a

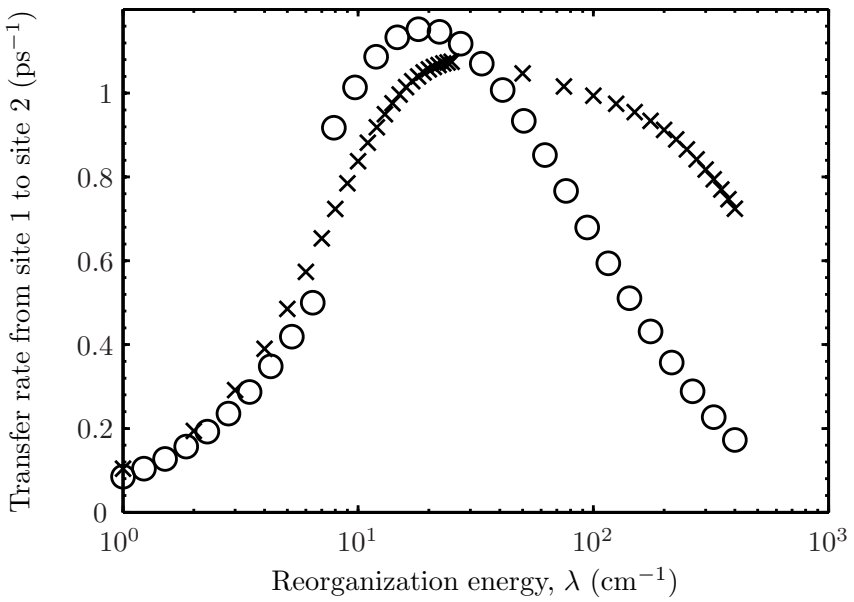

Figure 5-1: Rate of population transfer as a function of reorganization energy for a dimer with asymmetry $\Delta = 100$ cm^{-1}, coupling $J = 20$ cm^{-1}, ohmic spectral density as in Eq. (5.15) with inverse bath correlation time $\gamma = 100$ cm^{-1}, and temperature $T = 300$ K. The open circles are calculated by the variational minimization described in Chapter 4 while the crosses are calculated using the equilibrium technique in this chapter.

function of reorganization energy λ. The first thing that we observe about the results is that the discontinuous jump in rate that exists in the Gibbs–Bogoliubov results is absent from the equilibrium-optimized results. We also observe that the rates a large reorganization energy are increased by a factor of two or three.

Since the variational polaron transform was shown in Chapter 4 to perform very well at large reorganization energy, there is reason to be cautious of the results at large reorganization energy. The larger transfer rate is a direct result of the fact that the equilibrium coupling J_{eff} decreases rather slowly at large reorganization energy. Indeed, while the Gibbs–Bogoliubov minimization causes J_p to abruptly go to zero around $\lambda \approx 8$ cm^{-1}, the equilibrium minimization still has a $J_p = 6.8$ cm^{-1} at the largest reorganization energy considered, $\lambda = 400$ cm^{-1}.

Of course, the results of Lee et al. showing that the variational polaron transform produces approximately the correct equilibrium density matrix at large reorganization energy were only for superohmic spectral density $\eta(\omega) \sim \omega^3$. We next look at some

parameters similar to those examined by Lee et al. In particular, we use a superohmic spectral density

$$\eta(\omega) = \frac{\lambda}{2\pi}\frac{\omega^3}{\omega_c^3}e^{-\omega/\omega_c}, \tag{5.16}$$

where the cutoff frequency is $\omega_c = 0.75$. We consider a dimer with energy splitting $\Delta = 1$ and coupling $J = 3/2$, in units where $\hbar = \beta = 1$. In Fig. 5-2, we plot the energy transfer dynamics for several values of λ. The results follow the same general trend as in the ohmic case; for small to intermediate values of the system–bath coupling, there are some differences between the Gibbs–Bogoliubov and the equilibrium-optimized dynamics, but the overall rate of transfer is comparable. At large, system–bath coupling, however, the equilibrium-optimized dynamics predict a significantly larger transfer rate than the Gibbs–Bogoliubov dynamics. Just as in the ohmic case, this result is understandable by looking at the effective coupling, J_p, for the two transformations. For $\lambda = 15$, the Gibbs–Bogoliubov minimization results in J_p being effectively zero, while the equilibrium density matrix results in $J_{\text{eff}} = 0.2$. The much larger effective coupling in the equilibrium-optimized results is of course leading to the much larger transfer rate. Indeed, for both ohmic and superohmic spectral density, the effective coupling extracted from the equilibrium density matrix is much larger than the effective coupling obtained from the Gibbs–Bogoliubov bound.

5.4 Conclusion

This chapter briefly presented an alternative method of selecting a partial polaron transform to study quantum dynamics of the spin–boson Hamiltonian. In particular, we used the exactly known equilibrium reduced density matrix for the system to determine an effective Hamiltonian for the system; we then chose our polaron transform such that the resulting zeroth-order Hamiltonian approximated the effective Hamiltonian as closely as possible.

One of the motivations for exploring alternatives to the Gibbs–Bogoliubov choice of polaron transform was the presence of a discontinuous jump in energy transfer rates as a funcion of bath reorganization energy. While the method presented in

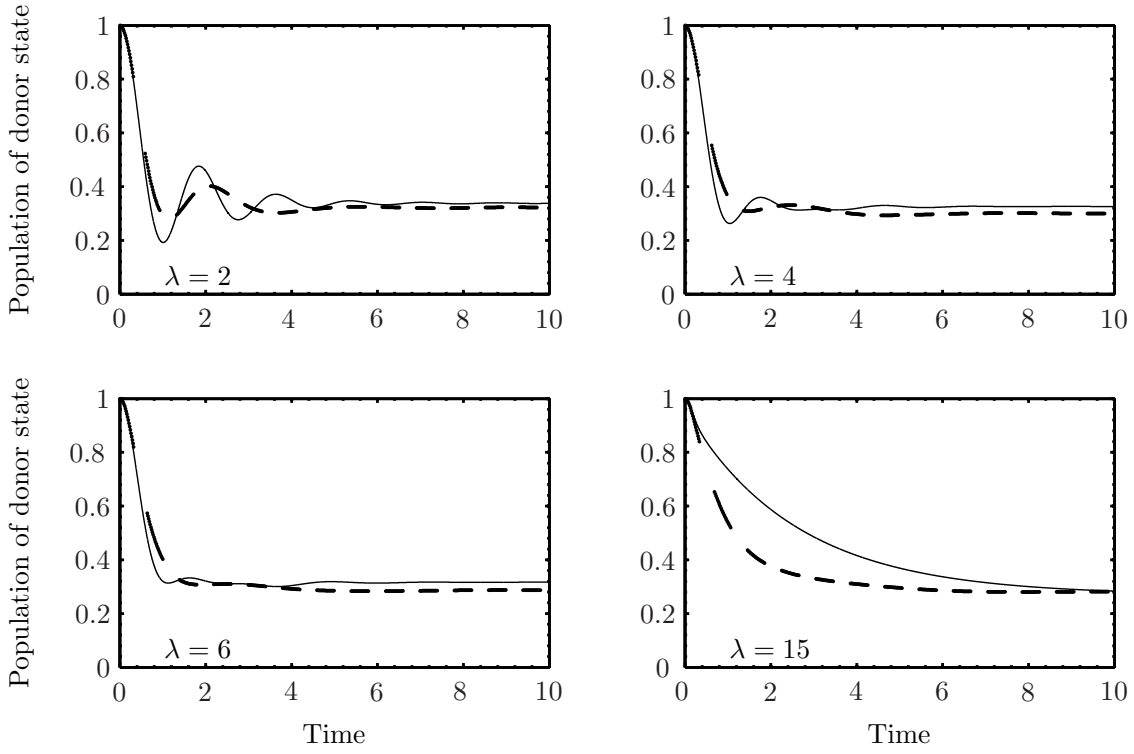

Figure 5-2: Population of donor state as a function of time for a dimer with splitting $\Delta = 1$ and coupling $J = 3/2$. The system is coupled to a bath with superohmic spectral density given by Eq. (5.16), with $\omega_c = 0.75$. The dynamics are plotted for four different values of the system–bath coupling λ, as indicated on each figure. Units are such that $\hbar = k_B T = 1$. The solid lines are calculated by the variational minimization described in Chapter 4 while the dashed lines are calculated using the equilibrium technique in this chapter.

this chapter does eliminate this jump, it appears to largely overestimate the rate of energy transfer at large system–bath coupling. This overestimation can be traced back to the fact that the effective coupling J_{eff} extracted from the equilibrium reduced density matrix is general much larger than the renormalized coupling J_p obtained from the Gibbs–Bogolioubov minimization. Thus, while it may be possible to find other ways of using equilibrium information to improve the variational transformation, the straightforward method presented here actually performs worse than the method in Chapter 4 when it comes to accurately predicting dynamics over a wide range of parameters.

Bibliography

[1] A. Ishizaki, T. R. Calhoun, G. S. Schlau-Cohen, and G. R. Fleming. Quantum coherence and its interplay with protein environments in photosynthetic electronic energy transfer. *Phys. Chem. Chem. Phys.* **12**, 7319 (2010).

[2] J. M. Moix, Y. Zhao, and J. Cao. Equilibrium-reduced density matrix formulation: Influence of noise, disorder, and temperature on localization in excitonic systems. *Phys. Rev. B* **85**, 115412 (2012).

[3] C. K. Lee, J. Moix, and J. Cao. Accuracy of second order perturbation theory in the polaron and variational polaron frames (2012). `arXiv:1201.2436v2 [quant-ph]`.

[4] V. Romero-Rochin and I. Oppenheim. Relaxation properties of two-level systems in condensed phases. *Physica A* **155**, 52 (1989).

[5] J. W. Allen and R. Silbey. Comments on exciton–phonon coupling. II. Variational solutions. *Chem. Phys.* **43**, 341 (1979).

Eric Zimanyi

Department of Chemistry
Massachusetts Institute of Technology
77 Massachusetts Avenue, Room 6-226
Cambridge, Massachusetts 02139-4307

Education

2012 (expected)	Ph.D. in Physical Chemistry Massachusetts Institute of Technology, Cambridge (Massachusetts)
2006	B. Sc. First Class Honours in Chemistry (Minor in Mathematics) McGill University, Montreal (Quebec)

Awards

2008–11	Doctoral Research Scholarship (FQRNT, Quebec government funding agency)
2006–08	Masters Research Scholarship (FQRNT)
2006	MIT Presidential Fellowship
2006	R. F. Robertson Award in Physical Chemistry (McGill University)
2006	Anne Molson Prize in Chemistry (McGill University)
2006	Sigma Xi Excellence in Undergraduate Research Award (McGill-Montreal chapter)
2005	Bellini Family Scholarship (McGill University)
2005	Undergraduate Student Research Award (NSERC, Canadian government funding agency)
2004	Alexander MacInnes Scholarship (McGill University)
2004	Undergraduate Student Research Award (NSERC)
2003	J. W. McConnell Scholarship (McGill University)
2003	Gold medal, 35th International Chemistry Olympiad, Athens (Greece)
2003	First place, Canadian Chemistry Olympiad, Kingston (Ontario)

Research

2007–2012	**Graduate Research Assistant, Massachusetts Institute of Technology** Supervisor: Prof. Robert Silbey
Summer 2005	**Undergraduate Research Associate, McGill University** Supervisor: Prof. David Ronis
Summer 2004	**Undergraduate Research Associate, McGill University** Supervisor: Prof. James Gleason

Peer-reviewed publications

Eric N. Zimanyi and Robert J. Silbey, *Theoretical Description of Quantum Effects in Multichromophoric Aggregates*, Phil. Trans. Roy. Soc. A. (2012). *In press.*

Eric N. Zimanyi and Robert J. Silbey, *Unified treatment of coherent and incoherent electronic energy transfer dynamics using classical electrodynamics*, J. Chem. Phys. **133**, 144107 (2010).

Eric N. Zimanyi and Robert J. Silbey, *The work-Hamiltonian connection and the usefulness of the Jarzynski equality for free energy calculations*, J. Chem. Phys. **130**, 171102 (2009). **Selected as an Editors' Choice article for 2009 by the Journal of Chemical Physics.**

Experience

2008–11 **Planning Committee, Greater Boston Theoretical Chemistry Seminars**

2008–09 **Co-president, MIT Chemistry Graduate Student Committee**

Fall 2006 **Teaching Assistant, Massachusetts Institute of Technology**
Course: 5.112, Principles of General Chemistry

2005–06 **Faculty of Science Committee, McGill University**

Skills

- Languages: English (native), French (fluent)
- Programming: C/C^{++}, Perl, Java, MATLAB, Mathematica